



저작자표시-비영리-변경금지 2.0 대한민국

이용자는 아래의 조건을 따르는 경우에 한하여 자유롭게

- 이 저작물을 복제, 배포, 전송, 전시, 공연 및 방송할 수 있습니다.

다음과 같은 조건을 따라야 합니다:



저작자표시. 귀하는 원저작자를 표시하여야 합니다.



비영리. 귀하는 이 저작물을 영리 목적으로 이용할 수 없습니다.



변경금지. 귀하는 이 저작물을 개작, 변형 또는 가공할 수 없습니다.

- 귀하는, 이 저작물의 재이용이나 배포의 경우, 이 저작물에 적용된 이용허락조건을 명확하게 나타내어야 합니다.
- 저작권자로부터 별도의 허가를 받으면 이러한 조건들은 적용되지 않습니다.

저작권법에 따른 이용자의 권리는 위의 내용에 의하여 영향을 받지 않습니다.

이것은 [이용허락규약\(Legal Code\)](#)을 이해하기 쉽게 요약한 것입니다.

[Disclaimer](#)

A Thesis for the Degree of Master of Science

**Identification of a Component of the Cellular
Secretion Pathway as an Interactor of a *Ralstonia*
solanacearum Type III Effector**

세포 분비 경로 단백질과 *Ralstonia solanacearum*
이펙터 단백질의 상호작용 구명

FEBRUARY, 2021

JEONGU LEE

**MAJOR IN HORTICULTURAL SCIENCE
AND BIOTECHNOLOGY
DEPARTMENT OF AGRICULTURE, FORESTRY AND
BIORESOURCES
SEOUL NATIONAL UNIVERSITY**

**Identification of a Component of the Cellular
Secretion Pathway as an Interactor of a *Ralstonia
solanacearum* Type III Effector**

**UNDER THE DIRECTION OF DR. CECILE SEGONZAC
SUBMITTED TO THE FACULTY OF THE GRADUATE SCHOOL
SEOUL NATIONAL UNIVERSITY**

**BY
JEONGU LEE**

**MAJOR IN HORTICULTURAL SCIENCE AND BIOTECHNOLOGY
DEPARTMENT OF AGRICULTURE, FORESTRY AND
BIORESOURCES
THE GRADUATE SCHOOL OF SEOUL NATIONAL UNIVERSITY**

FEBRUARY, 2021

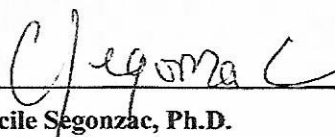
**APPROVED AS A QUALIFIED THESIS OF JEONGU LEE
FOR THE DEGREE OF MASTER OF SCIENCE
BY THE COMMITTEE MEMBERS**

CHAIRMAN



Doil Choi, Ph.D.

VICE-CHAIRMAN



Cecile Segonzac, Ph.D.

MEMBER



Jin Hoe Huh, Ph.D.

**Identification of a Component of the
Cellular Secretion Pathway as an Interactor of a
Ralstonia solanacearum Type III Effector**

JEONGU LEE

**DEPARTMENT OF AGRICULTURE, FORESTRY AND
BIORESOURCES
THE GRADUATE SCHOOL OF SEOUL NATIONAL UNIVERSITY**

ABSTRACT

Plants have innate immune responses against pathogens. Many bacterial pathogens secrete type III effectors (T3Es) to promote their growth. Thus, many T3Es target host defense-related components. Therefore, it is important to identify and characterize T3E interactors in the host plant. One bacterial pathogen, *Ralstonia solanacearum* (*R. solanacearum*) causes severe wilt in a wide range of horticultural crops. One of *R. solanacearum* T3E, RipAO, suppresses a defense response, namely flg22-triggered ROS production in *Nicotiana benthamiana*. Here, I screened *Arabidopsis thaliana* total cDNA library using RipAO to identify its interactors and test whether candidate interactors are required for the RipAO role to suppress flg22-ROS production. Using yeast two-hybrid screening, three candidate interactors, exocyst complex component SEC3A (SEC3A), SNF1 related protein kinase (KIN10), and *Arabidopsis thaliana* homolog of yeast oxidase assembly 1

(OXA1) were identified. Interestingly, SEC3A could not accumulate in the presence of RipAO. Moreover, RipAO could not or not fully suppress flg22-triggered ROS production in *N. benthamiana* plants silenced for SEC3A homologs. Taken together, these results suggest that RipAO targets the exocyst component SEC3A and that SEC3A is required for RipAO suppression of flg22-ROS production. Hence, this study uncovers a possible role of the vesicle trafficking machinery as the target of pathogen effectors to impair the host defense response.

Key Words: exocyst complex component SEC3A, SNF1 related protein kinase, *Arabidopsis thaliana* homolog of yeast oxidase assembly 1, yeast two-hybrid, reactive oxygen species, *Ralstonia solanacearum*, *Arabidopsis thaliana*, *Nicotiana benthamiana*

Student number: 2019-21592

CONTENTS

ABSTRACT	i
CONTENTS	iii
LIST OF TABLES	vi
LIST OF FIGURES	vii
LIST OF ABBREVIATIONS	x
INTRODUCTION	1
MATERIAL AND METHODS.....	5
Plant and yeast strain culture.....	5
Molecular cloning	5
Yeast two-hybrid system.....	7
<i>Agrobacterium tumefaciens</i> -mediated transient expression in <i>N. benthamiana</i>	9
Immunoprecipitation and immunoblotting.....	9
Virus induced gene silencing (VIGS) assay.....	11
Measurement of ROS production.....	11
Semi-quantitative RT-PCR.....	11

RESULTS	15
Selection of NLS-containing type III effectors.....	15
Cloning, expression and activity of the three selected effectors in yeast.....	16
Some <i>Arabidopsis thaliana</i> genes can activate <i>MEL1</i> gene with GAL4 DNA-binding domain.....	20
Yeast two-hybrid screening of <i>A. thaliana</i> cDNA library for RipAO interactors.....	23
Re-transformation of the original fished-out plasmids...	27
Cloning of full-length and truncated cDNA for candidate interactors of RipAO.....	29
Full-length and truncated candidate genes cannot activate <i>MEL1</i> gene with GAL4 DNA-activation domain.....	30
RipAO fused with GAL4 DNA binding-domain interacts with the full-length candidate fused with GAL4 DNA-activation domain.....	32
SEC3A-YFP accumulates less in the presence of RipAO-FLAG in <i>N. benthamiana</i>	35
Co-expression and co-IP assay of RipAO with KIN10 and OXA1.....	37

RipAO suppresses flg22-triggered ROS production in <i>N. benthamiana</i>	39
Design silencing fragment to knock-down candidate interactor homolog in <i>N. benthamiana</i>	41
ROS measurement in <i>N. benthamiana</i> silenced for SEC3A homolog and confirmation of silencing efficiency by semi-quantitative RT-PCR.....	45
Reactive oxygen species (ROS) measurement in <i>N. benthamiana</i> silenced for KIN10 homolog and confirmation of silencing efficiency by semi-quantitative RT-PCR.....	48
DISCUSSION	52
REFERENCES	59
ABSTRACT IN KOREAN	68

LIST OF TABLES

Table 1. List of primers

Table 2. List of autoactivating genes from the *A. thaliana* cDNA library used in this study

Table 3. List of genes identified in blue colonies as candidate RipAO interactors

LIST OF FIGURES

Figure 1. Expression of the effector-GAL4 binding domain fusion in yeast

Figure 2. Three studied Rips cannot activate the HIS3 reporter gene when co-expressed with GAL4 DNA activation-domain.

Figure 3. GAL4 DNA binding-domain interacts with some of *Arabidopsis* library proteins.

Figure 4. RipAO fused with GAL4 DNA binding-domain can activate *MEL1* gene when co-expressed with some *A. thaliana* proteins.

Figure 5. The original fished-out plasmids containing candidate gene fragments can activate the *MEL1* gene when co-expressed with RipAO fused with GAL4 DNA-binding domain in yeast.

Figure 6. Full-length and truncated *A. thaliana* candidate proteins cannot activate *MEL1* gene with GAL4 DNA activation-domain.

Figure 7. Some plasmids containing full-length candidate *A. thaliana* genes and truncated-SEC3A gene can activate the *MEL1* gene when co-expressed with RipAO fused with GAL4 DNA-binding domain in yeast.

Figure 8. The abundance of SEC3A is reduced in presence of RipAO in *N. benthamiana*.

Figure 9. KIN10-YFP is not interacting with RipAO-FLAG in *N. benthamiana*.

Figure 10. flg22-triggered ROS production is impaired presence of RipAO-YFP in *N. benthamiana*.

Figure 11. Amino acid sequence alignment of 2 NbSEC3A and AtSEC3A genes with silencing fragments

Figure 12. Amino acid sequence alignment of 4 NbKIN10 and AtKIN10 genes with silencing fragments

Figure 13. flg22-triggered ROS production in NbSEC3A homolog silenced *N. benthamiana* expressing RipAO

Figure 14. *NbSEC3A* expression in silenced *N. benthamiana*

Figure 15. *NbKIN10* expression in silenced *N. benthamiana*

Figure 16. flg22-triggered ROS production in 4 NbKIN10 homolog silenced *N. benthamiana* expressing effector

LIST OF ABBREVIATIONS

<i>A. thaliana</i>	<i>Arabidopsis thaliana</i>
<i>A. tumefaciens</i>	<i>Agrobacterium tumefaciens</i>
BLAST	Basic local alignment search tool
co-IP	co-immunoprecipitation
<i>E. coli</i>	<i>Escherichia coli</i>
EDS1	ENHANCED DISEASE SUSCEPTIBILITY1
ETI	Effector-triggered immunity
ETS	Effector-triggered susceptibility
FLS2	FLAGELLIN SENSING 2
GFP	Green fluorescent protein
HR	Hypersensitive response
KIN10	SNRK1 related protein kinase 1.1
LB	Luria-Bertani
MAPK	Mitogen-activated protein kinase
<i>N. benthamiana</i>	<i>Nicotiana benthamiana</i>
NB-LRR	Nucleotide-binding leucine-rich repeat

NLS	Nuclear localization signal
	<i>A. thaliana</i> homolog of yeast oxidase assembly
OXA1	1 protein
<i>P. syringae</i>	<i>Pseudomonas syringae</i>
PAD4	PHYTOALEXIN DEFICIENT4
PAMP	Pathogen-associated molecular pattern
PIP2	Phosphatidylinositol 4,5-bisphosphate
PM	Plasma membrane
PRR	Pattern recognition receptor
PTI	PAMP-triggered immunity
R gene	Resistance gene
<i>R. solanacearum</i>	<i>Ralstonia solanacearum</i>
Rip	<i>Ralstonia</i> injected protein
RLK	Membrane-bound receptor-like kinase
RLP	Receptor-like-protein
RLU	Relative light unit
ROS	Reactive oxygen species

<i>S. cerevisiae</i>	<i>Saccharomyces cerevisiae</i>
SD	Synthetic defined
semi qRT-PCR	Semi-quantitative RT-PCR
TF	Transcription factor
TGN/EE	<i>Trans</i>-Golgi network/early-endosome
TRV	Tomato Rattle Virus
VIGS	Virus induced gene silencing
<i>Xvc</i>	<i>Xanthomonas campestris</i> pv. <i>vesicatoria</i>
YFP	Yellow fluorescent protein
YPD	Yeast peptone dextrose

INTRODUCTION

Plants have a two-branched innate immune system to fend off pathogens (Jones and Dangl., 2006). The first branch of innate immunity is PAMP-triggered immunity (PTI) activated by recognition of pathogen-associated molecular patterns (PAMPs). PTI is initiated when the plasma membrane (PM) bound pattern recognition receptors (PRRs) detect PAMPs at the surface of the plants (Zipfel, 2014). PRRs mostly belong to the membrane-bound receptor-like kinase (RLKs) or receptor-like-protein (RLP) families (Zipfel, 2014). After perception of PAMP by PRRs, plants can initiate and activate the series of defense responses. PRRs form heterodimers with their co-receptors to initiate intracellular signaling that is required for defense responses. In the well-studied model plant *A. thaliana*, FLAGELLIN SENSING 2 (FLS2) recognizes the epitope flg22 of bacterial flagellin with BAK1 co-receptor (Chinchilla et al., 2007). Activation of PRRs induces various defense signaling and defense response events such as a burst of reactive oxygen species (ROS), callose deposition, increase of Ca^{2+} ion concentration, mitogen-activated protein kinase (MAPK) activation, and secretion of antimicrobials (Blume et al., 2000; Segonzac et al., 2011; Kadota et al., 2015). Protein transport to the target region and coordinated membrane dynamics are therefore involved in several plant immune mechanisms. For example, intracellular membrane vesicles can deliver defense proteins and compounds to the invasion site of pathogens as a directional movement (Bednarek et al., 2010). Moreover, the abundance of PRR on PM is also regulated by vesicle trafficking (Ben Khaled et al., 2015; Wang et al., 2020). Therefore, the vesicle trafficking of plant immunity related proteins to the right place as a dynamic

subcellular localization is critical for the plant immune responses (Ben Khaled et al., 2015).

On the other hand, successful plant pathogens can deploy virulence proteins called effectors to diminish plant defense responses causing effector-triggered susceptibility (ETS). For instance, one of well-studied *Pseudomonas syringae* (*P. syringae*) effectors, AvrPtoB, can suppress plant ROS production triggered by flg22 (Hann and Rathjen., 2007). In addition, another *P. syringae* effector HopAII targets MAPK and inactivates it through its phosphothreonine lyase activity (Zhang et al., 2007). However, in the second branch of plant immunity, the effectors can be specifically recognized by resistance (R) proteins in plants and trigger effector-triggered immunity (ETI). The *R* genes mostly encode intracellular nucleotide-binding leucine-rich repeat (NB-LRR) receptors. The initiation of ETI triggers similar responses as PTI but stronger and long-lasting which often brings a programmed cell death called hypersensitive response (HR) (Chiang and Coaker., 2015).

Ralstonia solanacearum (*R. solanacearum*) is a gram-negative bacterium that causes serious bacterial wilt disease in plants. Due to its extensive diversity and heterogeneous species, it is commonly called *R. solanacearum* species complex (RSSC) (Genin and Denny., 2012). *R. solanacearum* can inject a variety of effectors called Rips (*Ralstonia* injected proteins) or type III effectors (T3Es) by using their type III secretion system (T3SS) (Peeters et al., 2013; Genin., 2010). One of the most studied T3Es of *R. solanacearum* is PopP2 (RipP2) that localizes to the plant nucleus (Deslandes et al., 2003). PopP2 targets some defense signaling-related WRKY transcription factors of plants (Le Roux et al., 2015; Sarris et al., 2015). Another *R.*

solanacearum effector, RipAY is reported to be phosphorylated in the plants and is known to suppress PTI by mediating degradation of glutathione through its gamma-glutamyl cyclotransferase activity (Macho et al., 2017). Moreover, there are more than 100 effector families in RSSC (Genin and Denny., 2012). But most of the RSSC effector functions and the reason why it is possessing large numbers of effectors are still unknown.

In other phytopathogens, some effectors target vesicle trafficking to suppress PTI. For instance, *P. syringae* HopM1 can suppress PTI by targeting the *A. thaliana* trans-Golgi network/early-endosome (TGN/EE) associated AtMIN7 and mediates its degradation by the host 26S proteasome (Nomura et al., 2011). As AtMIN7 contributes to SA-regulated callose deposition, HopM1-mediated degradation of AtMIN7 weakens plant defense. Another *P. syringae* effector, AvrPtoB, ubiquitinates the exocyst subunit component EXO70B1 and mediates its degradation via the host 26S proteasome (Wang et al., 2019). EXO70B1 subunit is required for accumulation and homeostasis of FLS2 on PM (Wang et al., 2020). These findings are highlighting that effectors targeting vesicle trafficking have critical roles to suppress PTI.

In this study, I characterized one of *R. solanacearum* type III effectors, RipAO, which is reported to localize in the nucleus and in vesicles (Jeon et al., 2020). RipAO can suppress flg22-triggered ROS production and reduce flg22-induced defense gene expression (Jeon et al., 2020). In order to identify the interactors of RipAO, I performed yeast two-hybrid screening with *A. thaliana* whole cDNA library using yeast GAL4-based system. Individual candidate interactors were cloned into yeast expression vectors separately and confirmed in 1 to 1 interaction. Then I have

attempted to confirm the interactions in planta using co-immunoprecipitation (co-IP), but I discovered that RipAO might prevent the accumulation of one specific candidate. Finally, the function of RipAO in *N. benthamiana* was investigated in candidate interactors silenced plants. My results are organized into three parts:

1. Identification of RipAO targets in *A. thaliana* by yeast two-hybrid screening.
2. Confirmation of protein interaction between RipAO and candidate interactors by co-IP assay *in planta*.
3. Investigation of the role of RipAO interactors for its biological function by VIGS and ROS burst measurement.

This work is the first step for the characterization of *R. solanacearum* effector RipAO with its plant interactors. Further examination of RipAO with the interactors is necessary to help to understand the detailed mechanisms.

MATERIALS AND METHODS

Plant and yeast strain culture

N. benthamiana plants were grown for 5 to 6 weeks in a growth chamber at 24 to 26 °C and 60% relative humidity under a 16 h light/8 h dark cycle.

Saccharomyces cerevisiae (*S. cerevisiae*) strain Y187 and AH109 were provided by the Plant immunity laboratory at Pohang University of Science and Technology. Yeast strains were cultured in YPD broth (Takara) and maintained as glycerol stocks at – 80 °C in a deep-freezer. The library of *P. syringae*-infected *A. thaliana* cDNA inserted in the yeast expression vector pGADT7 in *S. cerevisiae* strain Y187 was kindly provided by professor Ho Won Jung, Dong-A University, Busan.

Molecular cloning

a) Construction of the bait vectors for the yeast-two-hybrid screen

Coding sequences of two *R. solanacearum* Type III effector RipAB and RipAF1 were amplified by PCR and ligated into the pGEMt_easy entry vector (Promega). RipAO coding sequence was synthesized by Genewiz and cloned into pUC57 vector. All the plasmids were mobilized into *Escherichia coli* (*E. coli*) DH5 α by electroporation. The coding sequence of each effector was confirmed by sequencing and subcloned into the restriction sites NdeI and NcoI (RipAB), NdeI and EcoRI (RipAF1), and EcoRI and BamHI (RipAO) of the yeast expression vector pGBKT7(GAL4-BD, bait). Each construct was then mobilized into *E. coli* DH5 α and confirmed by restriction enzyme digestion test. Confirmed vectors were transformed into yeast strain AH019 using Frozen-EZ Yeast Transformation II Kit

(Zymo Research) according to the manufacturer's protocol.

b) Construction of prey vectors to confirm yeast-two-hybrid screen results

Full-length and truncated coding sequence of *A. thaliana* SEC3A N-terminal (1-471aa), SEC3A C-terminal (471-892aa) Δ VAL654, SEC3A C-terminal (471-893aa), SEC3A Δ VAL654, SEC3A, SNRK1 related protein kinase 1.1 (KIN10) and *A. thaliana* yeast homolog of yeast oxidase assembly 1 protein (OXA1) were amplified by PCR from wild type *A. thaliana* Col-0 cDNA and cloned into pICH41021 vector. The coding sequences were then ligated into the yeast expression vector pGADT7(GAL4-AD, prey) through restriction sites SmaI and BamHI (SEC3A), and EcoRI and BamHI (SEC3A N-terminal, SEC3A C-terminal, KIN10, and OXA1). Then, each of the ligated plasmids was transformed into *E. coli* DH5 α . The vectors were confirmed by restriction enzyme digestion test and mobilized into *S. cerevisiae* Y187 strain using the Quick & Easy Yeast Transformation Mix (Takara). The transformants were stored as glycerol stock at -80°C.

c) Construction of binary vectors for in planta expression

Coding sequences of RipAO candidate interactors (SEC3A, KIN10, and OXA1) were amplified as about 1 kb-long golden gate compatible modules from *A. thaliana* Col-0 with BsaI site-flanking primers (Table 1). All the amplified fragments were ligated into the pICH41021 vector and confirmed by Sanger sequencing. Then the entry modules for each interactor candidate were assembled in fusion with C-terminal GFP under the control of the 35S promoter in the binary vector pICH86988, using BsaI-based Golden Gate assembly. Assembled constructs were confirmed by restriction analysis and mobilized to *Agrobacterium tumefaciens* (*A. tumefaciens*) AGL1 strain and stored as glycerol stock at -80°C.

d) Construction of silencing vectors

Two NbSEC3A homologs and 4NbKIN10 homologs were used for virus-induced gene silencing assay. Silencing fragments of 150 to 300 base pairs were designed for *N. benthamiana* homologs of AtSEC3A (*Niben101Scf00219g04018.1* and *Niben101Scf10412g01012.1*) and AtKIN10 (*Niben101Scf00063g05003.1*, *Niben101Scf04763g00007.1*, *Niben101Scf06026g00009.1* and *Niben101Scf17051g00006.1*) using Solgenomics.net (Sol Genomics Network). Each silencing fragment was PCR-amplified from the cDNA of wild type *N. benthamiana* and cloned into pICH41021 entry vector. Each silencing fragments was confirmed by sequencing. The silencing fragments were then ligated into the EcoRI and BamHI site of the pTRV2 vector. The constructs were confirmed by digestion test of restriction enzymes and transformed into *A. tumefaciens* AGL1 strain.

Yeast-two hybrid system

a) Selection of true bait transformants

Yeast transformants of AH109 having bait plasmid (pGBKT7) containing appropriate genes were selected on SD (synthetic drop-out) –Trp (lacking tryptophan). Selected yeast colonies were resuspended in potassium phosphate (67 mM) and lyticase solution containing 5 units/μl lyticase in 1X TE buffer (Sigma-Aldrich), digested at 37 °C for 30 to 60 minutes and used as PCR templates. To detect positive colonies, primers were designed to target 300 to 600 base pairs in the internal regions of effectors or interactor candidates in two yeast expression plasmids pGBKT7. Finally, to confirm the true transformants, plasmids were isolated from the positive colonies. Yeast cultures grown in appropriate SD medium for 18 to 24 h

were spin-down, digested in lyticase for 1h at 37°C, and resuspended in SDS (20%). Subsequently, plasmids were isolated with the QIAGEN miniprep kit (QIAGEN) according to the manufacturer's protocol. Isolated plasmids were re-transformed into *E. coli* and grown on LB (Luria-Bertani) broth containing appropriate antibiotics. Plasmids were isolated again and confirmed with a restriction enzyme digestion test.

b) Yeast two-hybrid screening using RipAO as a bait

To screen the candidates of effector interactors, two haploid strains, RipAO in AH109 and Y187 having *Arabidopsis* library were mated by incubation in 30°C for 24 to 30 hours in YPD (Yeast peptone dextrose) broth. Diploid yeasts containing both bait and prey plasmids were selected on SD –Trp-Leu-His-Ade (lacking tryptophan, leucine, histidine and adenine) medium. Selected diploid yeast colonies were re-streaked on SD –Trp-Leu-His-Ade + X- α -gal (5-Bromo-4-chloro-3-indolyl- α -D-galactopyranoside) medium. Subsequently, the yeast colony changed into blue, fished-out genes were amplified by colony PCR and confirmed by sequencing using primers of pGADT7 as described by Lu. 2011. The sequencing results were submitted to BLAST for identifying the gene.

c) Confirmation of one-to-one protein interaction between RipAO and full-length or truncated candidate interactors

Identified interactor genes were PCR-amplified and constructed in pGADT7 plasmids. Then, constructed plasmids were re-transformed into *S. cerevisiae* Y187 strain. The *S. cerevisiae* Y187 transformants containing prey plasmids were selected on SD –Leu medium. All the selected yeast transformants were confirmed by yeast colony PCR. Lastly, selected yeast transformants were grown together with *S. cerevisiae* AH109 strain containing bait plasmids for 24 to 30 h. Then, mated

diploids were serially diluted and dropped on SD –Trp-Leu-His-Ade + X- α -gal medium and SD –Trp–Leu medium in order to confirm whether the activation of *MEL1* gene is certainly due to the interaction between RipAO fused with GAL4-binding domain and candidate interactors fused with GAL4-activation domain.

***Agrobacterium tumefaciens*-mediated transient expression in *N. benthamiana*.**

To transiently express proteins in *N. benthamiana*, *A. tumefaciens* AGL1 cells containing plasmids with effector fused with 3xFLAG, and SEC3A, KIN10 and OXA1 fused with YFP were grown in LB broth containing appropriate antibiotics at 28°C for 24h. Cell cultures were spin-down and re-suspended to OD600 0.5 in infiltration medium (10 mM MgCl₂ and 10 mM MES-KOH, pH5.6). The infiltration was performed in the leaf of 5-6-week-old plants.

Immunoprecipitation and immunoblotting

a) Protein extraction from yeast

In order to test the protein expression in yeast, AH109 strain containing effectors in pGBKT7 were grown in appropriate SD media for 24 to 36 h and spin-down to be re-suspended in 100 μ l of sterilized distilled water to OD600 2.5. the resuspended pellet was treated with 0.2M NaOH and incubated at room temperature for 10 minutes. Then, the extracted total protein was spun-down to resuspend in a 3X loading buffer. Extracted protein with 3X loading buffer was boiled at 96°C for 3 minutes and loaded on a 10% acrylamide/bis-acrylamide gel.

b) Protein extraction from *N. benthamiana* leaves

Leaves of *N. benthamiana* expressing effector and interactor candidates were harvested 48 h after *A. tumefaciens* infiltration and frozen in liquid nitrogen. Leaves were ground to a fine powder in liquid nitrogen and resuspended in GTEN extraction buffer (10% glycerol, 150 mM Tris-HCl pH 7.5, 1 mM EDTA and 150 mM NaCl) containing cOmplete protease inhibitor (0.25 tablet / 10 ml), 1% Igepal detergent, 1% PVPP and 10 mM DTT (1, 4-Dithiothreitol). Total protein extract was mixed with 5X loading buffer containing 50 mM DTT in SDS loading dye (20% SDS, 10% glycerol, 0.5M Tris, and 18mg bromophenol blue), boiled at 96°C for 10 minutes, spin-down, and loaded on a 10% acrylamide/bis-acrylamide gel.

c) Immunoprecipitation from *N. benthamiana* total protein extract

Total protein extracts were incubated with anti-FLAG antibody-conjugated agarose beads (Sigma-Aldrich) overnight at 4°C. Beads were washed with washing buffer (10% glycerol, 150 mM Tris-HCl pH 7.5, 1 mM EDTA, and 150 mM NaCl) containing cOmplete protease inhibitor (0.25 tablet /10 ml), 1% Igepal detergent, and 10 mM DTT and boiled with 3X loading buffer at 96°C for 10 minutes. Immunopurified proteins were then separated on a 10% acrylamide/bis-acrylamide gel.

d) Western blotting

Proteins were transferred to the PVDD (polyvinylpolypyrrolidone) membrane in transfer buffer (20% Tris-Glycine and 10 % methanol) from the acrylamide gels. The membrane was blocked with 5% skim milk in TBST solution (Tris-buffered saline and 0.05% tween 20). Primary antibody (anti-FLAG Ab and anti-GFP Ab) and secondary antibody (anti-mouse HRP Ab) were diluted in 5% skim milk in TBST solution to 1/5,000 and 1/20,000 respectively. To detect the proteins on the

membrane, SuperSignal West Pico Chemiluminescent Substrate and SuperSignal West Femto Maximum Sensitivity Substrate (Thermo Scientific) were used as the manufacturer's instruction.

Virus induced gene silencing (VIGS) assay

To make *N. benthamiana* infected by TRV (Tomato Rattle Virus) and silence target genes, *A. tumefaciens* AGL1 cells carrying pTRV2 and pTRV1 plasmids were grown in the LB broth containing appropriate antibiotics for 24 h at 28 °C. Cells were spin-down, resuspended in infiltration medium (10 mM MgCl₂ and 10 mM MES-KOH, pH 5.6), and then infiltrated with a needleless syringe into the cotyledons of 2-week-old plants.

Measurement of ROS production

N. benthamiana leaf discs were harvested using a 5 mm diameter biopsy punch and floated overnight on 150 µl of sterilized water in 96 well-plates. The ROS production was measured by chemiluminescence. The water was replaced with 100 µl of assay solution (100 µM luminol (Sigma-Aldrich), 2 µg of horseradish peroxidase (Sigma-Aldrich), and 100 nM flg22 (Peptron)). The ROS burst was measured for 75 minutes using GloMax 96 Microplate Luminometer.

Semi-quantitative RT-PCR

N. benthamiana leaf discs used for the ROS measurement were collected and frozen in liquid nitrogen. Total RNA was extracted using TRIzol-Reagent (Ambion) and BCP (1-bromo 3-chloropropane; Sigma-Aldrich). Then, DNase I (Sigma-Aldrich)

was treated to extracted total RNA. First-strand cDNA was synthesized from 2.5 µg of RNA using Maxima first-strand cDNA synthesis kit (Thermofisher Scientific). Primer sets for semi-quantitative RT-PCR of NbSEC3A and NbKIN10 homologs were designed to target 150 to 300 base pairs in the internal region of each gene but outside the region used for silencing. The target regions were confirmed whether the set of primers are amplifying only the target regions by performing the BLAST using Solgenomics.net (Sol Genomics Network). 4µl of diluted cDNA was used as a semi-quantitative RT-PCR template. Then, the PCR products were loaded on 1.5% agarose gel. The transcription level of silenced genes by VIGS was quantified using ImageJ software, then normalized to the defense marker gene *NbEF1α* levels.

Table 1. List of primers

Gene/Plasmid	Sequence (5'→3')	Purpose
pGADT7	F : CTATTCGATGATGAAGATACCCCACCAAACCC	Sequencing
	R : AGTGAACCTGCGGGGTTTTTCAGTATCTACGAT	Sequencing
pGBKT7	F : TAATACGACTCACTATAGGGCGA	Sequencing
	R : CCTCAAGACCCGTTTAGAGG	Sequencing
RipAB	F : CATATGATGAGCCACAGCAAAATCAAGGC	Cloning
	R : CCATGGTCAGTCGTCGTCGTCCTTGATCTTC	Cloning
RipAF1	F : CATATGATGGGTTTGCCACGGATCCCC	Cloning
	R : GAATTCTCATCGCGTTGACGTGGA	Cloning
AtSEC3A	F : CCCGGAATGGCGAAATCAAGTGCTGA	Cloning
	R : GGATCCTTACATGGAAGCCAGAAGTCCT	Cloning
AtSEC3A_NT	F : GAATTCATGGCGAAATCAAGTGCTGA	Cloning
	R : GGATCCACGAGCCTCTCTACAAAGGAG	Cloning
AtSEC3A_CT	F : GTGAATTCGCGAATGAGCTTC	Cloning
	R : GGATCCTTACATGGAAGCCAGAAGTCCT	Cloning
AtKIN10	F : GAATTCATGGATGGATCAGGCACAGG	Cloning
	R : GGATCCTCATAGTACTCGGAGCTGAGC	Cloning
AtOXA1	F : GAATTCATGGCTTTCAGACAAACTTTATCTATA	Cloning
	R : GGATCCTCACTTCTTCTTGCTGCTATTCTT	Cloning
NbSEC3A_1, 2	F : GAATTCGAAAACAAAGCTGGTAAAAACACTG	Cloning
	R : GGATCCTATTCCATGCATTGATATACATCGC	Cloning
NbKIN10_1, 2	F : GAATTCGTGGGAGCAGCGTGGAGT	Cloning
	R : GGATCCTTTCCCTTCTCACTTTTTCTTCCATATCC	Cloning
NbKIN10_3	F : GAATTCATGACTAAAGAAGCCATAATTACAGA	Cloning
	R : GGATCCTTATCCAAAGGTTACTTGTACCAATG	Cloning
NbKIN10_4	F : GAATTCGGTAAAGTTAAAATTGCTGAGCATT	Cloning
	R : GGATCCTCCATCACAACATATATATCTGATG	Cloning

AtKIN10	F : GGTCTCAAATGGATGGATCAGGCACAGG	Cloning
	R : GGTCTCACCACCATGTTTCGATGGCAG	Cloning
	F : GGTCTCAGTGGTTCACAGAGATCTCAAGC	Cloning
	R : GGTCTCAACTCAGCCCCGAGATAACCA	Cloning
	F : GGTCTCAGAGTTTCAAGAAACCATGGAAGGT	Cloning
	R : GGTCTCACGAATAGTACTCGGAGCTGAGCAA	Cloning
AtOXA1	F : GGTCTCAAATGGCTTTCAGACAAACTTTATCTATA	Cloning
	R : GGTCTCACGAACTTCTTCTTGCTGCTATTCTTCTTC	Cloning
NbSEC3A_1, 2	F : AGTTTATCTGGGGTGGATAAGTCC	semi-qRT-PCR
	R : CGCATTCTGAGACAGATGGG	semi-qRT-PCR
NbKIN10_1, 2	F : TAAATTCAAGTGAAGCTGTTGC	semi-qRT-PCR
	R : CACTGAATTAGGTATAGGGAC	semi-qRT-PCR
NbKIN10_3	F : CACCAGTGTCACTGCCTCAA	semi-qRT-PCR
	R : GCGGATGATCTCCAGCAAGA	semi-qRT-PCR
NbKIN10_4	F : TGGTGTCACGATCTTGATTTTCC	semi-qRT-PCR
	R : AGAGGAACTGCGGACCACTA	semi-qRT-PCR

RESULTS

Yeast two-hybrid screening to identify the *Arabidopsis thaliana* proteins that interact with nuclear localization signal (NLS) –containing *Ralstonia solanacearum* Type III effector (T3E)

Selection of NLS-containing type III effectors

Some T3Es from phytopathogenic bacteria localize to the nucleus and play a crucial role to disrupt the defense signaling of the plants. 19 of 80 *R. solanacearum* effectors were predicted to carry a putative NLS (Jeon et al., 2020). Among these 19 effectors, several predicted NLS-containing T3Es showed suppression of flg22-induced ROS production in *N. benthamiana* (Jeon et al., 2020). One of NLS-containing T3Es, RipAO impairs total flg22-triggered ROS production in *N. benthamiana*. RipAF1 also delayed flg22-triggered ROS burst (Jeon et al., 2020). To link between immune-suppressive activity and effector subcellular localization, effectors were fused with a yellow fluorescent protein (YFP) and visualized by transient expression in *N. benthamiana* through the confocal microscopy assay. RipAB exclusively localized in the nucleus of the epidermal cell, RipAO localized to the nucleus and vesicles and RipAF1 is nucleocytoplasmic (Jeon et al., 2020). These 3 effectors were selected for further functional characterization.

Cloning, expression and activity of the three selected effectors in yeast

To understand how effectors affect plant immunity, we are looking for their target in the plant cell. Here I screened *A. thaliana* cDNA library with the yeast two-hybrid system to identify effector targets. The coding sequence of RipAB, RipAF1, and RipAO, were cloned under the control of the *ADHI* promoter into the yeast expression vector pGBKT7 using conventional restriction cloning. Confirmed constructs for the 3 effectors were obtained and mobilized into *S. cerevisiae* AH109.

In order to confirm the expression of effector-GAL4DB fusion in yeast, a western blot assay was performed (Figure 1). Total proteins of the *S. cerevisiae* AH109 containing each corresponding T3E-bait plasmid construct were extracted, resolved by electrophoresis through SDS-PAGE, and were immunoblotted with anti-Myc antibodies. ENHANCED DISEASE SUSCEPTIBILITY1 (EDS1) coding sequence constructed in the bait vector and pGBKT7 empty vector transformed *S. cerevisiae* AH109 cells were used as controls. RipAB, RipAF1, and RipAO fused with GAL4-binding domain were detected at around 40 kDa, 65 kDa, and 100 kDa respectively. The result indicates that all the effectors were well expressed and detected by immunoblotting.

To test the autoactivation activity of the effectors fused with the GAL4 DNA-binding domain, each *S. cerevisiae* AH109 transformants containing each effector-bait plasmid constructs were grown together with *S. cerevisiae* Y187 transformants containing pGADT7 (GAL4-activation domain) empty vector in YPD broth. Mated diploids containing EDS1 and PHYTOALEXIN DEFICIENT4 (PAD4) were constructed in the bait vector pGBKT7 and prey vector pGADT7 (Feys et al., 2001), and empty vector of pGBKT7 and pGADT7 plasmids were used as controls. Mated

diploids were ten-fold serial diluted and spotted to grow on SD -Trp-Leu and -Trp-Leu-His media (Figure 2). As a result of the test, each of the effectors fused with the GAL4 DNA-binding domain cannot activate the reporter gene (*HIS3*) conferring growth on medium lacking His with the GAL4 DNA-activation domain.

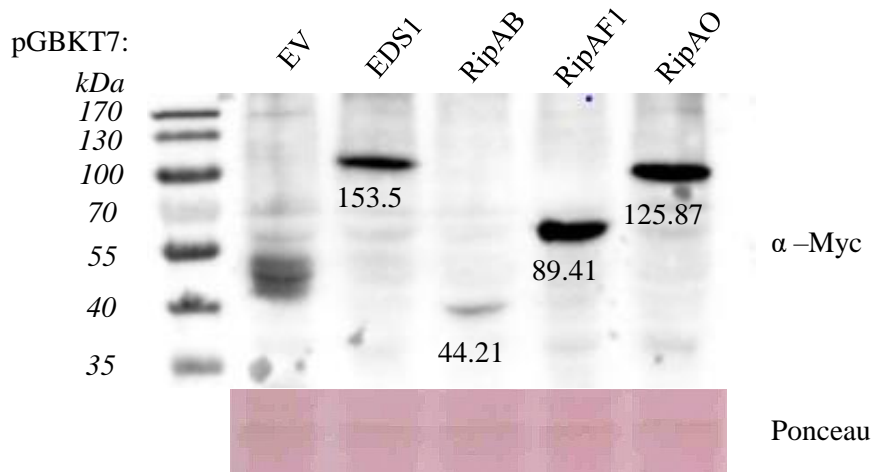


Figure 1. Expression of the effector-GAL4 binding domain fusion in yeast

SDS-PAGE and western blot analysis of each Rip expressed in yeast strain AH109 under the control of the *ADHI* gene promoter. pGBKT7 empty vector and *EDSI* constructed in pGBKT7 plasmid were used as a negative control and positive control, respectively. Yeast total protein was extracted, separated on acrylamide, and immunoblotted with anti-Myc antibodies. Numbers on each lane indicate the expected molecular sizes of each protein. Ponceau staining of the membrane attests to equal loading of proteins.

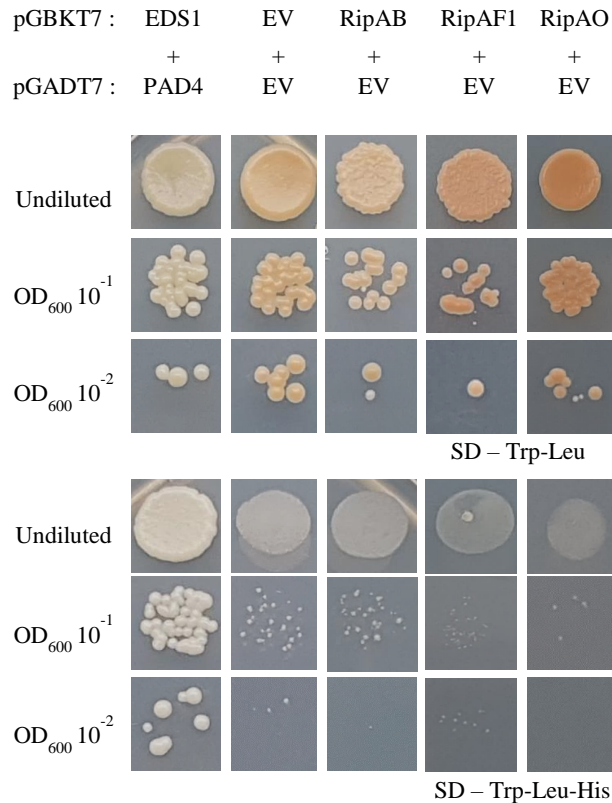


Figure 2. Three studied Rips cannot activate the *HIS3* reporter gene when co-expressed with GAL4 DNA activation-domain.

Mated diploids containing *ENHANCED DISEASE SUSCEPTIBILITY1* (*EDS1*) and *PHYTOALEXIN DEFICIENT4* (*PAD4*) constructed in bait and prey plasmid were used as a positive control. Mated diploids containing pGBKT7 and pGADT7 empty vectors were used as a negative control. Colonies grown on SD medium -Trp-Leu indicates that colonies are containing prey and bait plasmids and colonies grown on SD medium -Trp-Leu-His indicates bait-prey interaction between two proteins. Cells were grown on selective media for 5 days before photographs were taken.

Some *Arabidopsis thaliana* genes can activate *MEL1* gene with GAL4 DNA-binding domain

We hypothesized that some of the proteins from *A. thaliana* cDNA library may interact with the GAL4 DNA-binding domain. In order to leave out autoactivated library genes, a blank screening was performed. *S. cerevisiae* AH109 cells containing pGBKT7 empty vector was mated with *S. cerevisiae* Y187 transformants containing *A. thaliana* cDNA library constructed in pGADT7 plasmid. As a result of the blank screening, 12 different genes among 37 colonies were identified as genes that interact with the GAL4 DNA-binding domain (Figure 3, Table 2). Autoactivating genes were identified by colony PCR, sequencing, and the basic local alignment search tool (BLAST). Various proteins were revealed as interactors of the GAL4 DNA-binding domain including Ribosomal proteins, Calcium-binding EF-hand family proteins, and 26S proteasome AAA-ATPase subunit.

Table 2. List of autoactivating genes from the *A. thaliana* cDNA library used in this study

Gene	Description
AT1G70600.1	Ribosomal protein L18e/L15 superfamily protein
AT1G10350	DNAJ heat shock family protein
AT1G18210.1	Calcium-binding EF-hand family protein
AT5G62300.1	Ribosomal protein S10p/S20e family protein
AT4G20362.1	ATRA8D, ATRAB1B, RAB GTPASE HOMOLOG E1B, RAB1B, SUPPRESSOR OF VARIATION11, SVR11
AT3G47833.1	SDH7, SDH7A, SUCCINATE DEHYDROGENASE 7
AT5G20000	AAA-type ATPase family protein

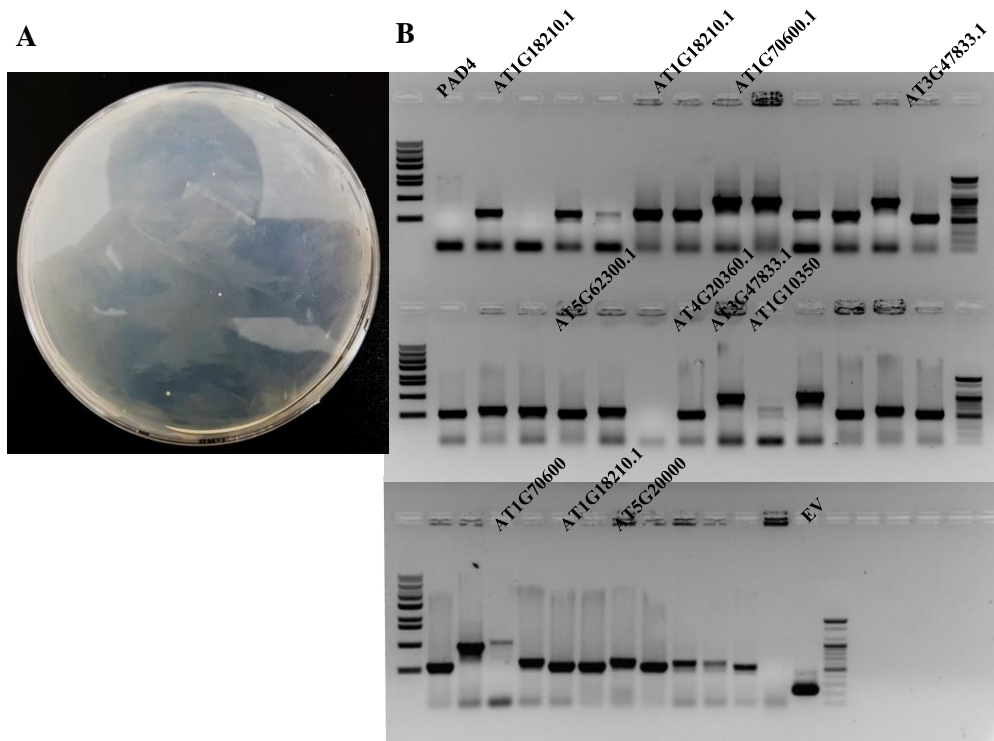


Figure 3. GAL4 DNA binding-domain interacts with some of *Arabidopsis* library proteins

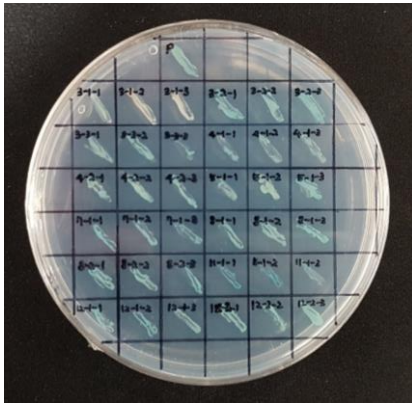
(A) *S. cerevisiae* mated diploids containing empty pGBKT7 plasmid and cDNA library constructed in pGADT7 plasmids were mated and grown on SD medium –Trp-Leu-His-Ade. 37 colonies grew on selective medium A representative plate was photographed after 5 days at 30C.

(B) Colony PCR assay of colonies from SD medium –Trp-Leu-His-Ade showed bands of different sizes. PCR-amplification was performed using primers targeting the internal region of pGADT7 plasmid which the cDNA fragment is inserted. Mated diploids containing pGADT7:PAD4 and pGBKT7:EDS1, and pGADT7 EV and pGBKT7 EV were used as controls (EV and PAD4 respectively). Band size for pGADT7:PAD4 and pGADT7 EV is 1847 bp and 221 bp respectively.

Yeast two-hybrid screening of *A. thaliana* cDNA library for RipAO interactors

To identify proteins that interact with RipAO, *S. cerevisiae* AH109 transformants containing RipAO-GAL4 DNA-binding domain constructed in pGBKT7 plasmid were grown together with *S. cerevisiae* Y187 transformants containing *A. thaliana* cDNA library constructed in pGADT7 plasmid and spotted on selective interaction medium. Through this screening, a total of 31 colonies grew out on SD-THLA. To eliminate false-positive, I first re-streak each colony on SD –Trp-Leu-His-Ade medium to perform colony segregation. Then I picked 3 colonies (total 96 colonies from 31 original colonies) for each and grew them on SD –Trp-Leu-His-Ade + x- α -gal medium again to confirm whether the colonies are turning blue. Then I performed yeast colony PCR to amplify the RipAO candidate interactors. Through the yeast colony PCR analysis, I could observe 28 colonies giving an identical band of about 1.2 kb (Figure 4), 2 colonies giving a band about 0.9 kb, and 1 colony giving a band of about 0.4 kb from the total 31 colonies (Table 3). PCR products were gel purified and sent for sequencing confirmation to identify the sequence of interactors through BLAST in TAIR (www.arabidopsis.org) and National Center for Biotechnology Information (www.ncbi.nlm.gov) website. The result indicated that the 1.2 kb bands all contained cDNA fragment of the exocyst complex component SEC3A, the bands of about 0.9 kb encoded SNF1 kinase homolog 10 (AtKIN10) and the band of about 0.4 kb was a cDNA fragment of *A. thaliana* oxidase homolog of yeast assembly 1 protein (OXA1).

A



B

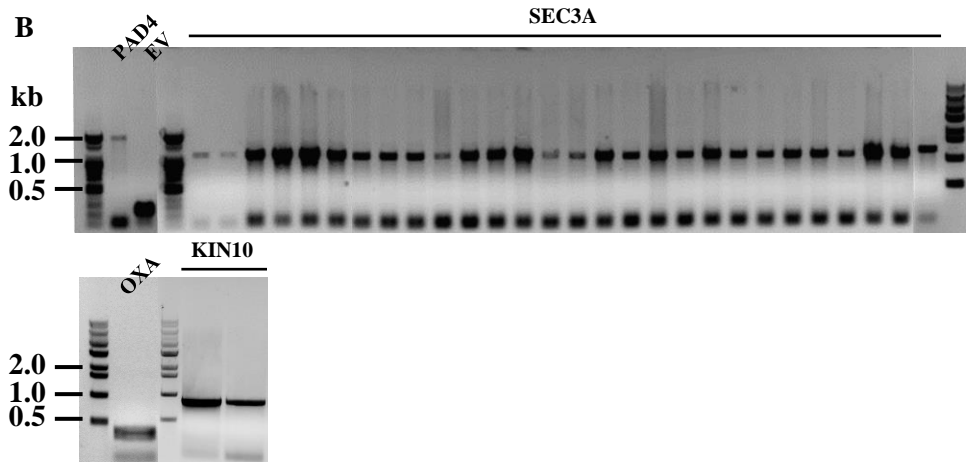


Figure 4. RipAO fused with GAL4 DNA binding-domain can activate *MEL1* gene when co-expressed with some *A. thaliana* proteins

(A). *S. cerevisiae* mated diploids grew on the SD –Trp-Leu-His-Ade + x- α -gal medium. Mated diploids containing pGADT7:PAD4 and pGBKT7:EDS1 were used as a positive control (P). Colonies were grown on the SD –Trp-Leu-His-Ade medium were re-streaked for segregation analysis on the SD –Trp-Leu-His-Ade + x- α -gal medium. Blue color indicates that bait and prey plasmids in diploids can activate the *MEL1* gene. A representative plate with 12 original colonies re-streak was photographed after 5 days at 30C.

(B). Colony PCR products of 31 colonies from the screening. 28 identical band sizes of about 1.2 kb, 2 identical band sizes of about 0.9 kb, and 1 band size of about 0.4 kb are corresponding to SEC3A, KIN10, and OXA1 cDNA fragments respectively. Mated diploids containing pGADT7:PAD4 and pGBKT7:EDS1, and pGADT7 EV and pGBKT7 EV were used as controls (EV and PAD4 respectively). PCR was performed with primers of pGBKT7 plasmid as described by Lu. 2011. Band size for pGADT7:PAD4 and pGADT7 EV is 1847 bp and 221 bp respectively.

Table 3. List of genes identified in blue colonies as candidate RipAO interactors

Gene	Description	Protein length (AA)	Number of colonies
AT1G47550	Exocyst complex component SEC3A	889	28
AT3G01090	KIN10, SNF1 related protein kinase	513	2
AT5G62050	<i>Arabidopsis thaliana</i> homolog of yeast oxidase homolog	430	1

Confirmation of RipAO full-length and truncated candidate interactors by one-to-one interaction through yeast two-hybrid assay

Re-transformation of the original fished-out plasmids

Plasmids were isolated from the identified colonies and retransformed into the *S. cerevisiae* Y187 strain in order to confirm whether the activation of the *MELI* gene is indeed due to the presence of the fished-out plasmids. *S. cerevisiae* AH109 transformants containing RipAO-GAL4 DNA-binding domain and each Y187 strain containing candidate plasmids were grown together in YPD broth and dropped to grow on SD medium –Trp–Leu–His–Ade + X- α -gal and SD medium –Trp–Leu. As a result of the test, I could observe that plasmids from original colonies can activate the *MELI* gene (Figure 5) as the mated diploids turned blue. This demonstrates that the plasmids isolated from the original colonies contain specific interactors of RipAO.

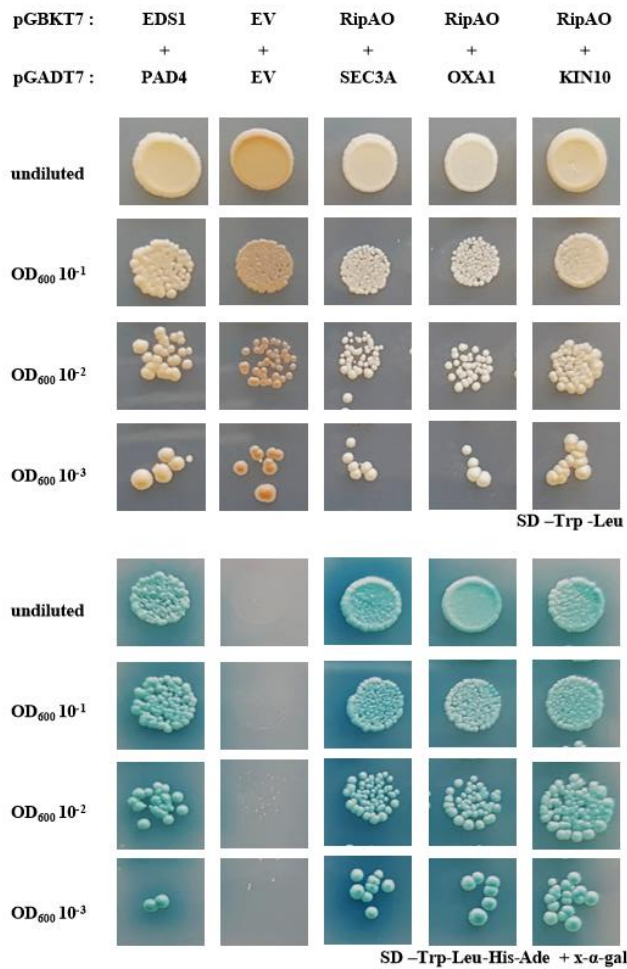


Figure 5. The original fished-out plasmids containing candidate gene fragments can activate the *MEL1* gene when co-expressed with RipAO fused with GAL4 DNA-binding domain in yeast.

Interaction test between RipAO-DNA-binding domain and *A. thaliana* cDNA fragments fused with GAL4 DNA-activation domain. Colonies growing on SD – Trp–Leu contains pairs of prey and baits plasmids. The blue color of colonies on SD –Trp–Leu–His–Ade + x-a-gal medium indicates activation of *MEL1* genes due to protein interaction. Mated cells were grown for 6 days at 30°C before photographs were taken.

Cloning of full-length and truncated cDNA for candidate interactors of RipAO

The cDNA fragments isolated from the yeast two-hybrid screening are partial, lacking the 5' region that encodes the N-terminal part of proteins, and had about 300aa (about 589-889aa). To test if the full-length SEC3A, KIN10, and OXA1 proteins interact with RipAO, the entire open reading frame of the candidate were amplified and cloned into the pGADT7 yeast expression vector. Moreover, in order to test which region of SEC3A would interact with RipAO, I generated truncated SEC3A fragments that encode N-terminal(1-471aa) containing phosphatidylinositol 4,5-bisphosphate (PIP2) domain and SEC3A C-terminal(471-889aa) (<https://www.ebi.ac.uk/interpro/>). Interestingly, while I was amplifying the full-length cDNA of SEC3A, I found two types of sequence: one matches with known *Arabidopsis* reference while the other one is lacking the 654th Valine. The cDNA fragments that I could isolate from the screening did not contain 654th Valine. Thus, I generated constructs of SEC3A (Δ Val 654) and SEC3A C-terminal (Δ Val 654) in pGADT7 plasmid, in order to identify whether RipAO interacts with both forms of SEC3A.

Full-length and truncated candidate genes cannot activate *MEL1* gene with GAL4 DNA-activation domain

I hypothesized that some of the cloned genes may activate the *MEL1* gene with the GAL4 DNA-binding domain, thus, they may be false positives. Therefore, to leave out autoactivated genes, I first performed an autoactivation test prior to perform a one-to-one interaction test with *S. cerevisiae* AH109 strain containing RipAO in bait plasmid. In order to test this, *S. cerevisiae* Y187 strain containing full-length and truncated candidate gene cloned in pGADT7 were individually grown together with *S. cerevisiae* AH109 strain containing pGBKT7 EV in YPD broth for 24 h. For the controls, mated diploids containing EDS1 and PAD4 constructed in the bait vector pGBKT7 and prey vector pGADT7 (Feys et al., 2001), and empty vector of pGBKT7 and pGADT7 plasmids were used, respectively. The mated diploids were serially diluted and dropped on SD -Trp-Leu and -Trp-Leu-His-Ade+x- α -gal media (Figure 6). As a result of the test, mated diploids could only grow on SD -Trp-Leu medium. This indicates that each of the full-length and truncated candidate genes fused with the GAL4 DNA-activation domain cannot activate the *MEL1* gene with the GAL4 DNA-binding domain. This result is in accordance with none of the three candidates being identified on the blank screen.

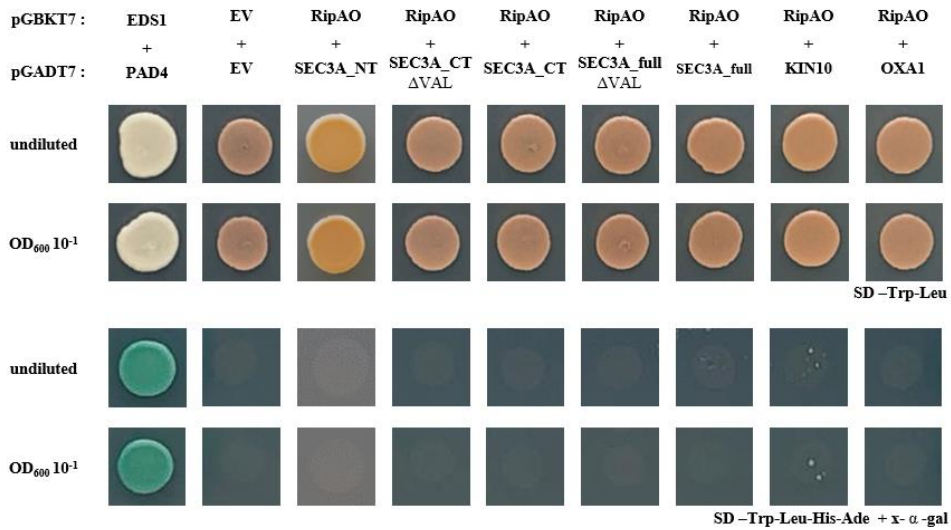


Figure 6. Full-length and truncated *A. thaliana* candidate proteins cannot activate *MEL1* gene with GAL4 DNA activation-domain

Interaction test between GAL4 DNA-binding domain and full-length and truncated *A. thaliana* candidate proteins fused with GAL4 DNA-activation domain. Colonies growing on SD –Trp–Leu contains pairs of prey and baits plasmids. The blue color of colonies on SD –Trp–Leu–His–Ade + x-α-gal medium indicates activation of *MEL1* genes due to protein interaction. Mated cells were grown for 5 days at 30°C before photographs were taken.

RipAO fused with GAL4 DNA binding-domain interacts with the full-length candidate fused with GAL4 DNA-activation domain

In order to examine whether RipAO is interacting with three full-length and truncated candidate interactors, I performed a yeast two-hybrid assay. *S. cerevisiae* AH109 strain containing RipAO constructed in pGBKT7 plasmid and *S. cerevisiae* Y187 strain containing each of full-length and truncated genes cloned in pGADT7 plasmid were grown together individually in YPD broth for 24 h. The mated diploids were serially diluted to spot on SD –Trp–Leu, SD –Trp–Leu–His, and SD –Trp–Leu–His–Ade + x- α -gal media. As a result of the yeast two-hybrid assay, I could observe that RipAO fused with the GAL4 DNA-binding domain can activate *MEL1* genes with both SEC3A and SEC3A (Δ Val 654), and KIN10 fused with the GAL4 DNA-activation domain (Figure 7). Also, I could observe RipAO fused with GAL4 DNA-binding domain can activate the *MEL1* gene with the C-terminal region of SEC3A fused with GAL4 DNA-activation domain, but not with the N-terminal region (Figure 7). Finally, mated diploids containing construct of RipAO in pGBKT7 and OXA1 in pGADT7 could not grow on SD –Trp–Leu–His–Ade + x- α -gal medium but could grow on SD –Trp–Leu–His. Taken all together, this indicates that RipAO can interact with SEC3A independently of the presence of 654th Valine and that RipAO can specifically interact with the C-terminal region of SEC3A but not with the N-terminal region. In addition, RipAO interacts with KIN10 and OXA1 but has weaker interaction with OXA1.

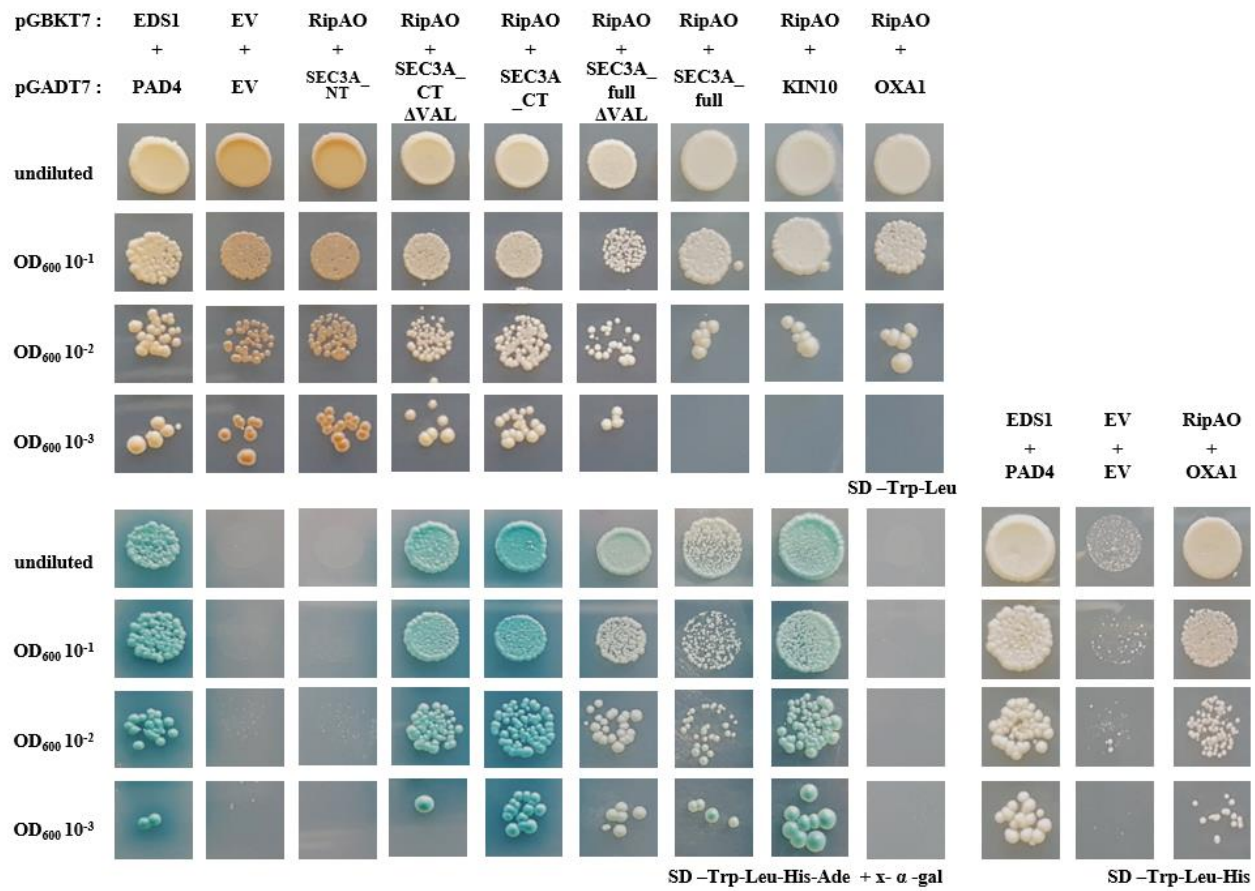


Figure 7. Some plasmids containing full-length candidate *A. thaliana* genes and truncated-SEC3A gene can activate the *MEL1* gene when co-expressed with RipAO fused with GAL4 DNA-binding domain in yeast

Interaction test between RipAO-DNA-binding domain and, full-length and truncated *A. thaliana* cDNA fused with GAL4 DNA-activation domain. Colonies growing on SD –Trp–Leu contains pairs of prey and bait plasmids. The blue color of colonies on SD –Trp-Leu-His-Ade + x-a-gal medium indicates activation of *MEL1* genes due to protein interaction. Colonies growing on SD –Trp–Leu–His indicates the activation of *HIS3* genes due to the weak protein interaction. Mated cells were grown for 6 days at 30°C before photographs were taken.

Testing the interaction between RipAO and candidate interactors in *planta*

SEC3A-YFP accumulates less in the presence of RipAO-FLAG in *N. benthamiana*

In order to test whether RipAO and SEC3A are interacting *in planta*, RipAO-3xFLAG and SEC3A-YFP were co-expressed in *N. benthamiana* leaves through *Agrobacterium*-mediated transient expression. The well-studied *R. solanacearum* effector PopP2 (Sarris et al., 2015) fused with 3xFLAG-tag was co-expressed with SEC3A-YFP as a negative control. RipAO-FLAG and GFP were co-expressed as another negative control. Total proteins were extracted from leaves infiltrated with different *Agrobacterium* density and examined by immunoblotting using anti-GFP and anti-FLAG antibodies. SEC3A-YFP was detected by the anti-GFP antibody when co-expressed with PopP2-3xFLAG. However, the accumulation of SEC3A-YFP co-expressed with RipAO-FLAG was significantly lower and decreased with increasing accumulation of RipAO-3xFLAG (Figure 8). This result indicates that SEC3A cannot accumulate in the presence of RipAO.

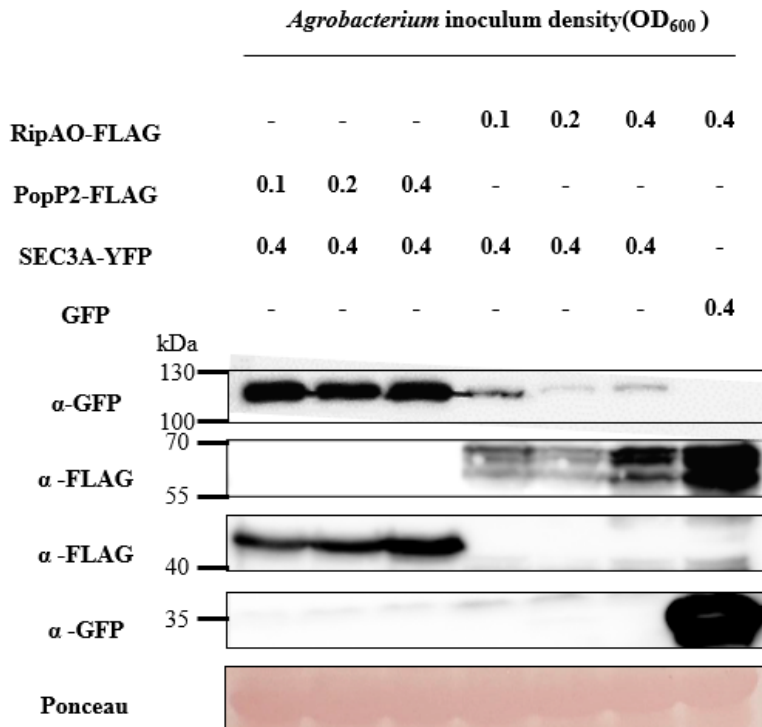


Figure 8. The abundance of SEC3A is reduced in presence of RipAO in *N. benthamiana*

A western blot assay of total protein extracts *N. benthamiana* leaf co-expressing SEC3A-YFP or GFP with different amounts of RipAO-3xFLAG or PopP2-3xFLAG. Proteins were separated by SDS-PAGE and detected by using anti-FLAG or anti-GFP antibodies. *Agrobacterium* inoculum density for SEC3A-YFP and GFP expression was adjusted to OD₆₀₀ 0.4, and co-infiltrated with different amount of RipAO/PopP2-3xFLAG of OD₆₀₀ 0.4, 0.2, and 0.1. Total proteins from *N. benthamiana* leaf were extracted after 48h after infiltration. The expected molecular weights of each protein are 26.4kDa (GFP), 127kDa (SEC3A-YFP), 50.01kDa (RipAO-3xFLAG), and 53.86 kDa (PopP2-3xFLAG). Ponceau staining of the membrane attests to equal loading of proteins. This experiment was conducted twice with a similar result.

Co-expression and co-IP assay of RipAO with KIN10 and OXA1

To test if RipAO and two other interactors, KIN10 and OXA1 are associated, I first co-expressed them in *N. benthamiana*. FLAG-tagged RipAO with YFP-tagged KIN10 and OXA1 was respectively co-expressed in *N. benthamiana*. RipAO-FLAG with LIP5 fused with YFP (Interaction between RipAO-FLAG and LIP5-YFP was confirmed by Hyelim Jeon through co-IP assay) were co-expressed for positive control, PopP2-FLAG with LIP5-YFP or GFP were used as negative controls. Then total proteins were extracted, and an immunoblotting assay was performed with anti-FLAG and anti-GFP antibodies. The level of KIN10-YFP was detected as much as LIP5-YFP did but OXA1-YFP was not detected by the anti-GFP antibody (Figure 9). In order to confirm whether KIN10-YFP and RipAO-FLAG are interacting with each other, the co-IP assay was performed. RipAO-FLAG and PopP2-FLAG were immunoprecipitated with anti-FLAG antibody-conjugated beads. Anti-GFP antibody could detect only LIP5-YFP co-expressed with RipAO-FLAG but KIN10-YFP was not detected in both RipAO-FLAG and PopP2-FLAG co-expressed leaves (Figure 9). This indicates that KIN10-YFP may not interact with RipAO-YFP.

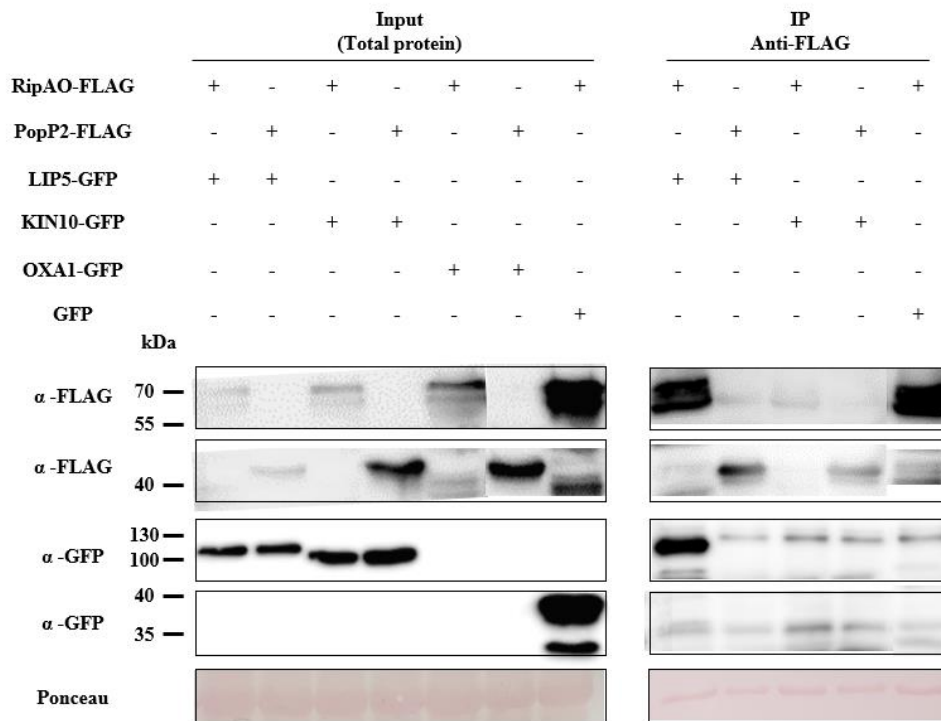


Figure 9. KIN10-YFP is not interacting with RipAO-FLAG in *N. benthamiana*

A western blot assay of total protein of KIN10-YFP / OXA1-YFP and RipAO-3xFLAG were transiently co-expressed in *N. benthamiana*. Leaf. LIP5-YFP with RipAO-3xFLAG / PopP2-3xFLAG and GFP with RipAO-3xFLAG were used for controls. Total proteins from *N. benthamiana* leaf were extracted after 48h after infiltration. Total protein extracts were subjected to anti-FLAG IP before immunoblotting using anti-FLAG or anti-GFP antibodies. The expected molecular weights of each protein are 26.4kDa (GFP), 85.28kDa (KIN10-YFP), 47.87kDa (OXA1-YFP), 73.12kDa (LIP5-YFP), 50.01kDa (RipAO-3xFLAG), and 53.86kDa (PopP2-3xFLAG). Ponceau staining attests to equal loading. This experiment was conducted three times with similar results.

RipAO requires the candidate interactors to suppress flg22-triggered ROS production in *Nicotiana benthamiana*

RipAO suppresses flg22-triggered ROS production in *N. benthamiana*

To confirm that RipAO can suppress flg22-triggered ROS production in *N. benthamiana*, RipAO-YFP was transiently expressed before ROS production measurement. AvrPtoB, a T3E from *Pseudomonas syringae* pv. *tomato* which suppresses flg22-triggered ROS production (Hann and Rathjen., 2007) and GFP were used as a positive and negative control respectively. Infiltrated leaf disks were harvested at 1 dpi and treated with flg22 to measure the flg22-triggered ROS production for 75 minutes. Compared to the flg22-triggered ROS production in GFP expressing leaf, the flg22-triggered ROS production was significantly reduced in both RipAO and AvrPtoB expressing leaf (Figure 10). But flg22-triggered ROS production in RipAO-expressing leaf was not reduced as much as flg22-triggered ROS production in AvrPtoB-expressing leaf. This result indicates that RipAO-YFP can suppress ROS production in *N. benthamiana*.

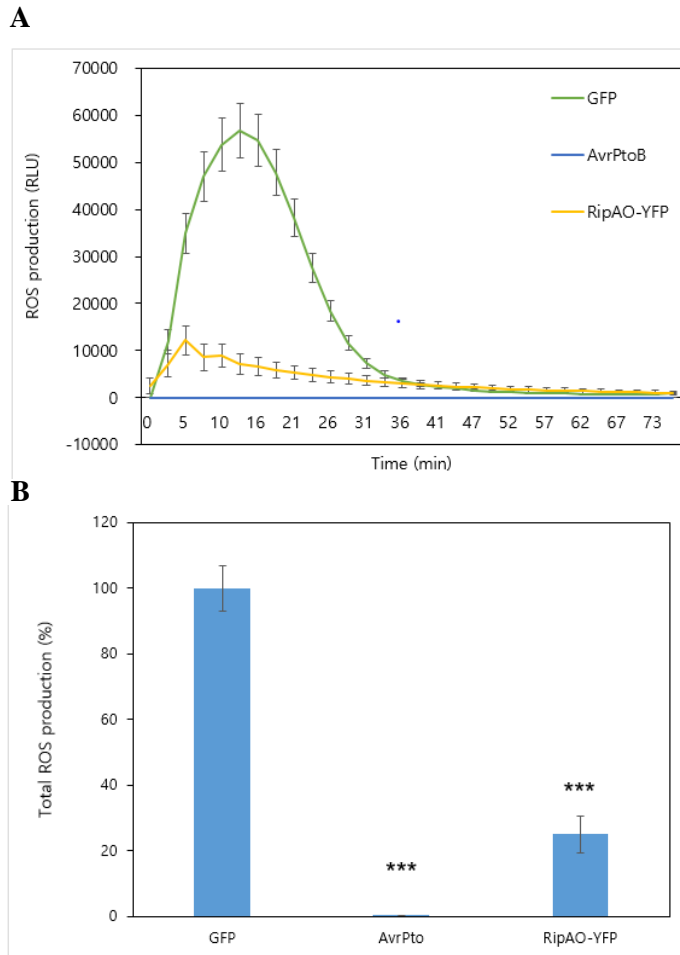


Figure 10. flg22-triggered ROS production is impaired presence of RipAO-YFP in *N. benthamiana*

Flg22-induced ROS burst was measured for 75 min in *N. benthamiana* leaf disks. GFP and AvrPtoB were included as negative and positive control respectively. (A) kinetic of ROS production following elicitation with flg22. (B) Total ROS production for 75 min was presented as relative (%) to GFP control. Data shown in (A-B) are means \pm SEM ($n=16$) from one experiment. Statistical significance compared to the GFP-expressing leaf is indicated by asterisks in (B) (Student's t-test, *** $p<0.001$). RLU, relative light unit.

Design silencing fragment to knock-down candidate interactor homolog in *N. benthamiana*

Since RipAO showed suppression of flg22-triggered ROS production in *N. benthamiana*, we hypothesized that RipAO may require the candidate interactors for this function. Therefore, VIGS assay using a TRV-based vector was employed to silence the expression of SEC3A and KIN10 homologs in *N. benthamiana* prior to RipAO expression and ROS measurement. First, I identified *N. benthamiana* SEC3A and KIN10 homologs using the database in Solgenomics.net (Sol Genomics Network). One silencing fragment was generated to target the two *N. benthamiana* SEC3A homologs (NbSEC3A_1 and NbSEC3A_2) due to the high percentage of identity of two homologs (Figure 11). Also, three silencing fragments were derived from the four *N. benthamiana* KIN10 homologs (NbKIN10_1, NbKIN10_2, NbKIN10_3, and NbKIN10_4) (Figure 12). Due to the high percentage of identity in NbKIN10_1 and NbKIN10_2, one DNA fragment was derived and theoretically designed for silencing both homologs. Then, a VIGS assay on *N. benthamiana* was performed by *A. tumefaciens* containing each silencing fragment inserted in the pTRV2 vector (TRV:NbSEC3A_1-2, TRV:NbKIN10_1-2, TRV:NbKIN10_3, and TRV:NbKIN10_4).

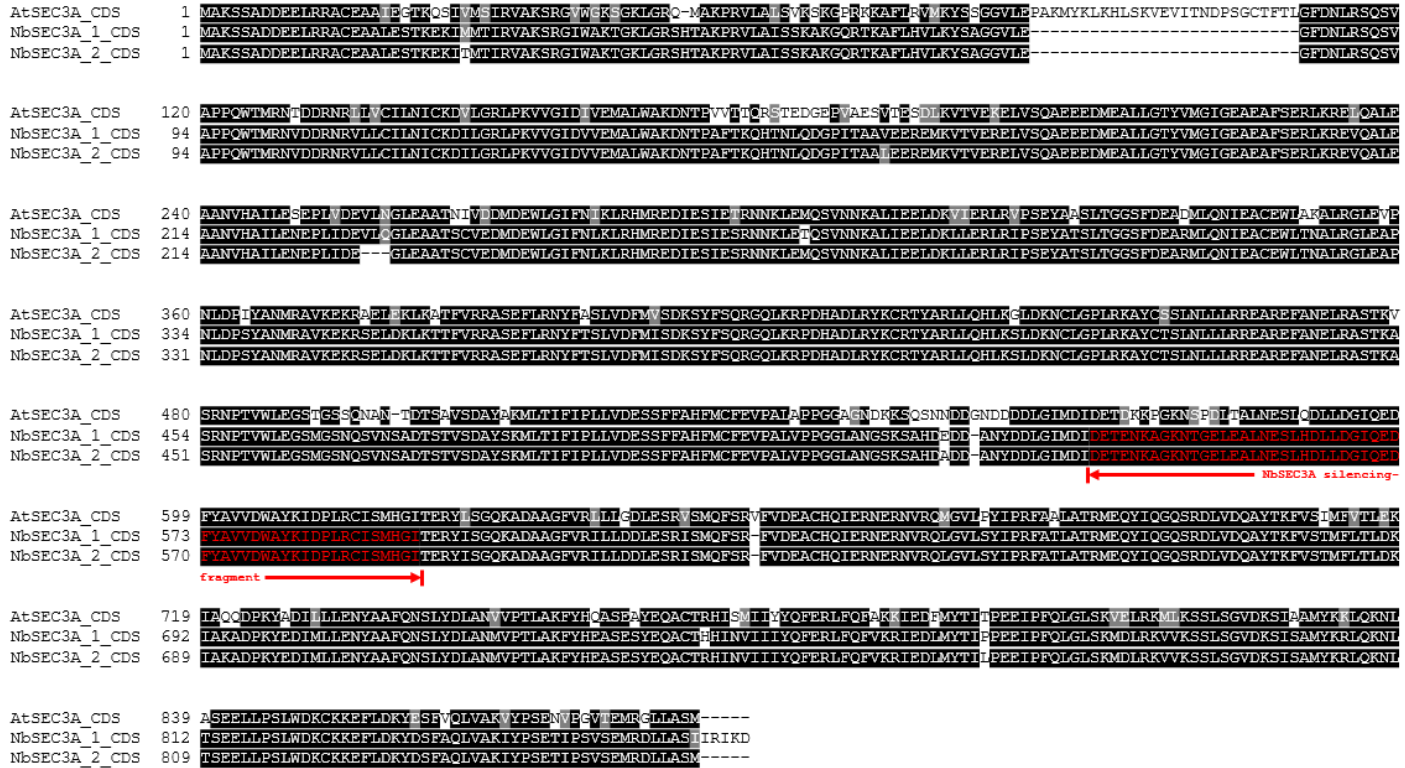


Figure 11. Amino acid sequence alignment of 2 *NbSEC3A* and *AtSEC3A* genes with silencing fragments

Homologs of SEC3A in *A. thaliana* and *N. benthamiana* amino acid sequence alignment using Clustal Omega and BoxShade.

Red indicates the location of the silencing fragment.

AtKIN10_CDS	1	MDGSGTGSRSQVESIIENYKLGKTLGIGSGFKVKIAEHLTGHKVAVKILNRRKIKNMDEEKVRRREIKILRLEFMHPHIIRLYEVIETPSDIYVMEYVNSGELFDYIVEKGRLEDEAR
NbKIN10_1_CDS	1	MDGSTVQCGSSVESFLRNYKLGKTLGIGSGFKVKIAEHLTGHKVAVKILNRRKIKNMDEEKVRRREIKILRLEFMHPHIIRLYEVIETPSDIYVMEYVNSGELFDYIVEKGRLEDEAR
NbKIN10_2_CDS	1	MDGSTVQCGSSVESFLRNYKLGKTLGIGSGFKVKIAEHLTGHKVAVKILNRRKIKNMDEEKVRRREIKILRLEFMHPHIIRLYEVIETPSDIYVMEYVNSGELFDYIVEKGRLEDEAR
NbKIN10_3_CDS	1	MDGSTVQSSSSVDSFLRNYKLGKTLGIGSGFKVKIAEHLTGHKVAVKILNRRKIKNMDEEKVRRREIKILRLEFMHPHIIRLYEVIETPSDIYVMEYVNSGELFDYIVEKGRLEDEAR
NbKIN10_4_CDS	1	--MSRGGCGITDTPFLRNYRLEKTLGIGSGFKVKIAEHLTGHKVAVKILNRRKIKNMDEEKVRRREIKILRLEFMHPHIIRLYEVIETPSDIYVMEYVNSGELFDYIVEKGRLEDEAR
AtKIN10_CDS	121	NFFQOIIISGVEYCHRNMVVHRDLKPENLLDLSKQNVKIADFGLSNIMRDGHFLKTS CGSPNYAAPEVISGKLYAGPEVDVWSCGVILYALLCGTLPFDDENI PNLFKKIKGGYITLPSHL
NbKIN10_1_CDS	121	NFFQOIIISGVEYCHRNMVVHRDLKPENLLDLSKQNVKIADFGLSNIMRDGHFLKTS CGSPNYAAPEVISGKLYAGPEVDVWSCGVILYALLCGTLPFDDENI PNLFKKIKGGYITLPSHL
NbKIN10_2_CDS	121	NFFQOIIISGVEYCHRNMVVHRDLKPENLLDLSKQNVKIADFGLSNIMRDGHFLKTS CGSPNYAAPEVISGKLYAGPEVDVWSCGVILYALLCGTLPFDDENI PNLFKKIKGGYITLPSHL
NbKIN10_3_CDS	121	NFFQOIIISGVEYCHRNMVVHRDLKPENLLDLSKQNVKIADFGLSNIMRDGHFLKTS CGSPNYAAPEVISGKLYAGPEVDVWSCGVILYALLCGTLPFDDENI PNLFKKIKGGYITLPSHL
NbKIN10_4_CDS	119	NFFQOIIISGVEYCHRNMVVHRDLKPENLLDLSKQNVKIADFGLSNIMRDGHFLKTS CGSPNYAAPEVISGKLYAGPEVDVWSCGVILYALLCGTLPFDDENI PNLFKKIKGGYITLPSHL
AtKIN10_CDS	241	SFGARDLIPRMLIVDPMKRTIPEIRNHPWFQAHLPRLYLAVPPDDTMOQAKKIDEEILQEVVVRMGFDRNSLIESLNRRVQNEGTVA YYLLLDNRFRASSGYLGAEFQETMECTPRHPA
NbKIN10_1_CDS	241	SAGARDLIPRMLIVDPMKRTIPEIRNHPWFQAHLPRLYLAVPPDDTMOQAKKIDEEILQEVVVRMGFDRNSLIESLNRRVQNEGTVA YYLLLDNRFRASSGYLGAEFQETMEYGYHQINSS
NbKIN10_2_CDS	241	SAGARDLIPRMLIVDPMKRTIPEIRNHPWFQAHLPRLYLAVPPDDTMOQAKKIDEEILQEVVVRMGFDRNSLIESLNRRVQNEGTVA YYLLLDNRFRASSGYLGAEFQETMEYGYHQINSS
NbKIN10_3_CDS	241	SAGARDLIPRMLIVDPMKRTIPEIRNHPWFQAHLPRLYLAVPPDDTMOQAKKIDEEILQEVVVRMGFDRNSLIESLNRRVQNEGTVA YYLLLDNRFRASSGYLGAEFQESVEYGYNRRNNSN
NbKIN10_4_CDS	239	SAGARDLIPRMLIVDPMKRTIPEIRNHPWFQAHLPRLYLAVPPDDTMOQAKKIDEEILQEVVVRMGFDRNSLIESLNRRVQNEGTVA YYLLLDNRFRASSGYLGAEFQESMDGYSPGTFPN
AtKIN10_CDS	360	ESVASPVSHLPGIMDYQVCGAROFFVERKQWALGQSRAPREIMTEVLKALQGLNVRWKKIGCPYNMKQWVPCVSGHHEGMSNNSIN--NFFGDDSTVIENGCVI--IENAVKFEVQLY
NbKIN10_1_CDS	361	EAVASPVG--HLPGIMDYQVCGAROFFVERKQWALGQSRAPREIMTEVLKALQGLNVRWKKIGCPYNMKQWVPCVSGHHEGMSNNSIN--NFFGDDSTVIENGCVI--IENAVKFEVQLY
NbKIN10_2_CDS	361	EAVASPVGHLPGIMDYQVCGAROFFVERKQWALGQSRAPREIMTEVLKALQGLNVRWKKIGCPYNMKQWVPCVSGHHEGMSNNSIN--NFFGDDSTVIENGCVI--IENAVKFEVQLY
NbKIN10_3_CDS	361	EAVTSPVQRYPGIMDYQVCGAROFFVERKQWALGQSRAPREIMTEVLKALQGLNVRWKKIGCPYNMKQWVPCVSGHHEGMSNNSIN--NFFGDDSTVIENGCVI--IENAVKFEVQLY
NbKIN10_4_CDS	359	LDIQLSTCN-----GISQEANLRHPSKDKKLLVGLQSPANPREIMTEVLKALQGLNVRWKKIGCPYNMKQWVPCVSGHHEGMSNNSIN--NFFGDDSTVIENGCVI--IENAVKFEVQLY
AtKIN10_CDS	478	KTRDEKYLDDLQRVQGPQFLFLDLCAAFLAQLRVI-----
NbKIN10_1_CDS	477	KTREEKYLDDLQRVQGPQFLFLDLCAAFLAQLRVI-----
NbKIN10_2_CDS	478	KSREEKYLDDLQRVQGPQFLFLDLCAAFLAQLRVI-----
NbKIN10_3_CDS	480	KTREEKYLDDLQRVQGPQFLFLDLCAAFLAQLRVI-----
NbKIN10_4_CDS	469	KRPDEKYLDDLQRLSGPQFLFLDLCAAFIMOLEBAPQ-----
AtKIN10_CDS		-----
NbKIN10_1_CDS		-----
NbKIN10_2_CDS		-----
NbKIN10_3_CDS	600	GFDLNDISVTASKGTFVLVTSMSVEVVRGGLIEAHQIREILLEIIRGI
NbKIN10_4_CDS		-----

Figure 12. Amino acid sequence alignment of 4 *NbKIN10* and *AtKIN10* genes with silencing fragments

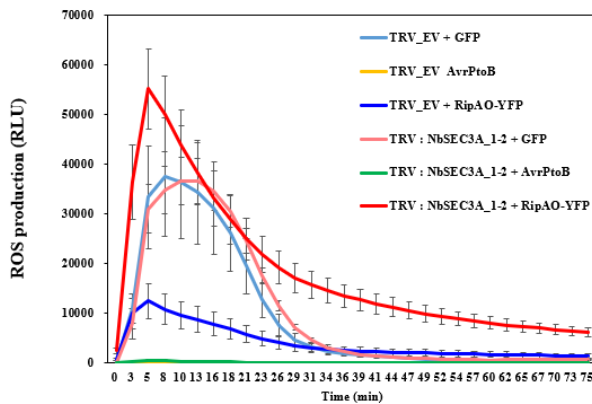
Homologs of KIN10 in *A. thaliana* and *N. benthamiana* amino acid sequence alignment using Clustal Omega and BoxShade. The red arrow indicates the location of the silencing fragment.

ROS measurement in *N. benthamiana* silenced for SEC3A homolog and confirmation of silencing efficiency by semi-quantitative RT-PCR

The RipAO suppression of flg22-triggered ROS burst was tested in TRV:EV and TRV:SEC3A1-2 plants. GFP and AvrPtoB were used as negative and positive controls respectively. Leaf disks from silenced plants were harvested at 1dpi and ROS production was measured for 75 minutes after treatment of flg22. First of all, flg22-triggered ROS production in both GFP expressed TRV:EV and TRV:SEC3A1-2 plants are similar (Figure 13A). Also, I could not observe that suppression of flg22-triggered ROS production in AvrPtoB expressed leaf in both TRV:EV and TRV:SEC3A1-2 plants was impaired. Finally, the flg22-triggered ROS production was not suppressed or less suppressed by RipAO-YFP compared to TRV:EV plants (Figure 13B).

In order to confirm that both SEC3A homologs were successfully silenced in TRV:SEC3A1-2 plants, I first extracted the total RNA from the leaf disks after the measurement of flg22-ROS production. Then, cDNA was synthesized from the extracted RNA. The cDNA was amplified by using the housekeeping gene *NbEF1 α* and *NbSEC3A1-2* specific primers. The band intensity of the PCR products of two *NbSEC3A* on the agarose gel was quantified using ImageJ software and normalized by the *NbEF1 α* gene. The experiment was repeated independently 3 times. The relative expression level of two *NbSEC3A* amount was reduced over 80% than the TRV:EV plants (Figure 14A-B). Together, these results indicate that one or the two *NbSEC3A* homologs are associated with ROS production triggered by flg22 and that one or the two *NbSEC3A* are required for RipAO to impair ROS production triggered by flg22.

A



B

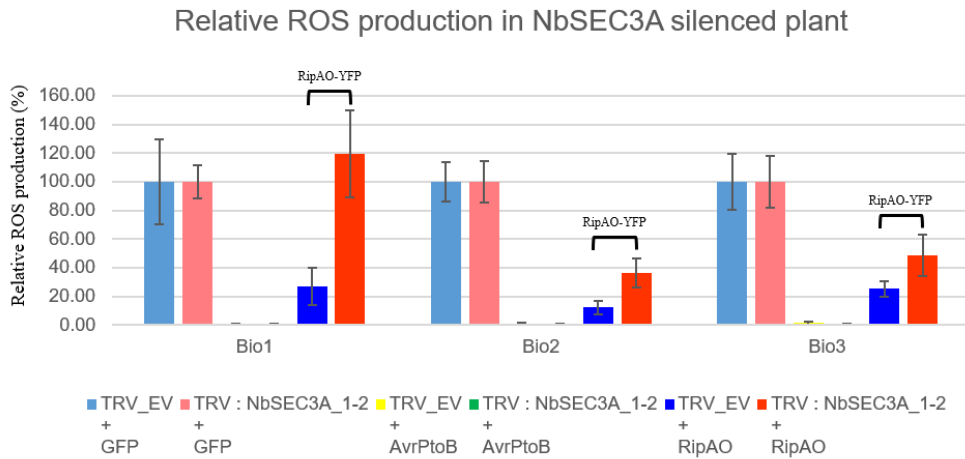


Figure 13. flg22-triggered ROS production in NbSEC3A homolog silenced *N. benthamiana* expressing RipAO

Flg22-induced ROS burst was measured for 75 min from *N. benthamiana* leaf disks. GFP control and AvrPtoB were included as negative and positive control respectively. (A) kinetic of ROS production following elicitation with flg22. (B) Total ROS production for 75 min was presented as relative (%) to GFP control. Data shown in the graph are means \pm SEM ($n=16$) from one (A) and three (B) independent experiments. RLU, relative light unit.

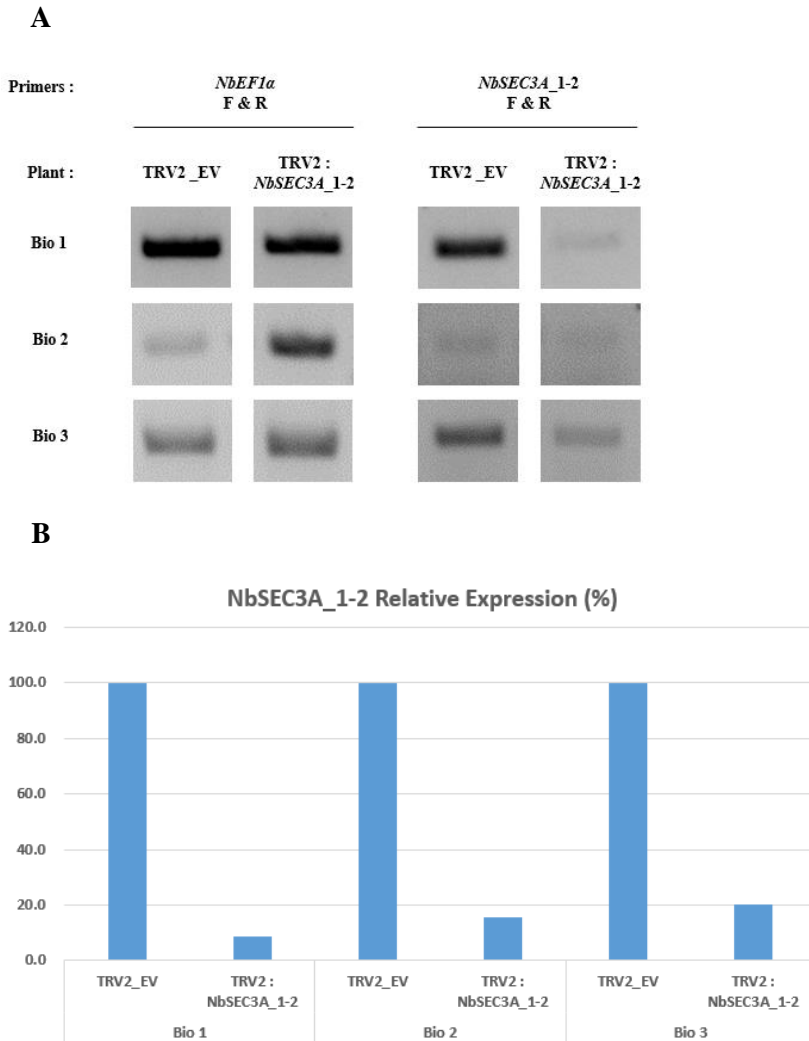


Figure 14. *NbSEC3A* expression in silenced *N. benthamiana*

(A). Semi-q RT-PCR was used to determine the intensity of *NbSEC3A* silencing. Amplicons obtained with EF1 α and SEC3A primers after 22 and 25 cycles were resolved on 1.5% agarose gel. The results of 3 independent biological repeats are shown. (B). Quantification of *NbSEC3A* relative expression levels shown in (A) using ImageJ software. All the samples were normalized by quantified *NbEF1 α* shown in (A).

Reactive oxygen species (ROS) measurement in *N. benthamiana* silenced for KIN10 homolog and confirmation of silencing efficiency by semi-quantitative RT-PCR

Prior to the test the RipAO suppression of flg22-triggered ROS burst, I first generated 3 types of *KIN10* silenced *N. benthamiana* (TRV:KIN10_1-2, TRV:KIN10_3 and TRV:KIN10_4) with TRV:EV plant for control. To confirm whether the NbKIN10 homologs were successfully silenced, total RNA was extracted from the leaf disks used for the ROS measurement (figure 15). Then cDNA was synthesized and amplified by using housekeeping gene *NbEF1 α* and silencing gene-specific primers. The band intensity was quantified from the PCR products on agarose gel using ImageJ software. Each of NbKIN10 homologs in *N. benthamiana* was not successfully suppressed in TRV:NbKIN10_1-2, TRV:NbKIN10_3, and TRV:NbKIN10_4 plants (Figure 15A-C). However, I could confirm that all four *NbKIN10* genes were partially silenced in TRV:NbKIN10_4 plants in Bio1 (Figure 15A).

Therefore, I compared the result of the test of RipAO suppression of flg22-triggered ROS burst in TRV:EV and TRV:KIN10_4 plants in Bio1. GFP and AvrPtoB were used as negative and positive controls respectively. Leaf disks from silenced plants were harvested at 1dpi and ROS production was measured for 75 minutes after treatment of flg22. AvrPtoB expressed leaves from both TRV:EV and TRV:NbKIN10_4 plants showed suppressed flg22-triggered ROS production (Figure 16). But in GFP expressed leaf from TRV:NbKIN10_4 plant showed reduced flg22-triggered ROS production compare to GFP expressed leaf from TRV:EV. Finally, in TRV:NbKIN10_4 plant from Bio1, RipAO-YFP did not show reduced suppression or any other remarkable difference of the flg22-trigger ROS production

compare to RipAO-YFP expressed leaf from TRV:EV (Figure 16A-C). This result may indicate that RipAO does not requires NbKIN10 homologs to suppress flg22-triggered ROS production or maybe NbKIN10 homologs are not silenced.

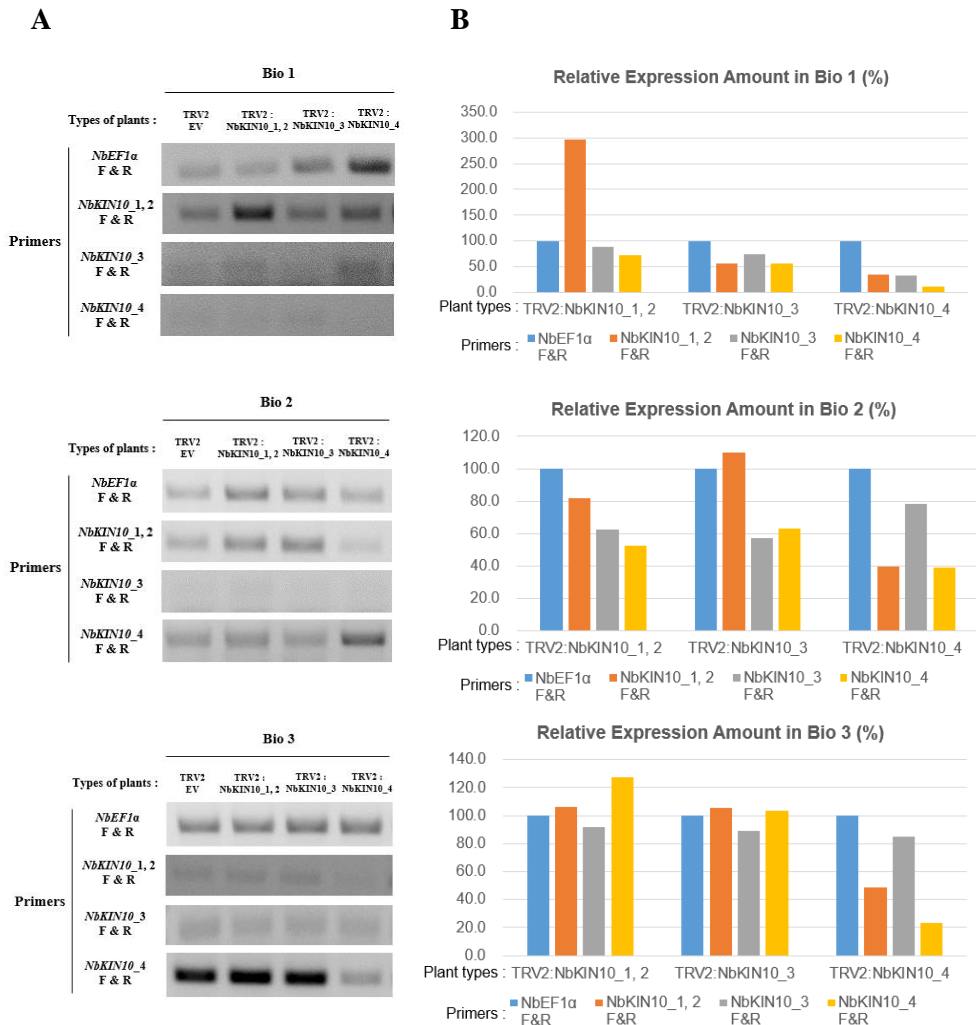


Figure 15. *NbKIN10* expression in silenced *N. benthamiana*

(A). Semi-q-RT-PCR was used to determine the intensity of *NbSEC3A* silencing. Amplicons obtained with EF1α, NbKIN10_1-2, NbKIN10_3, and NbKIN10_4 specific primers after 22, 27, 23, and 27 cycles respectively, were resolved on 1.5% agarose gel. The results of 3 independent biological repeats are shown. (B). Quantification of *NbKIN10* relative expression levels shown in (A) using ImageJ software. All the samples were normalized by quantified *EF1α* shown in (A)

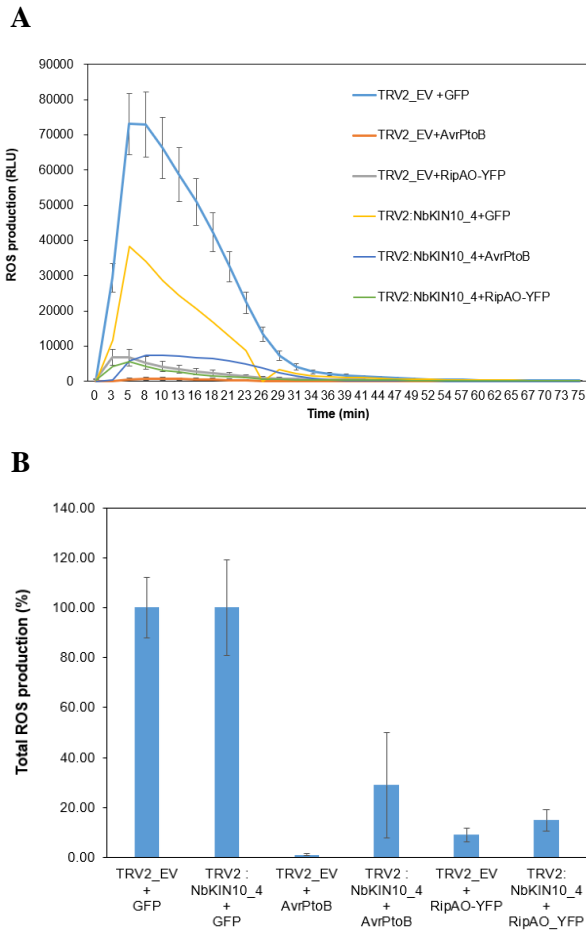


Figure 16. flg22-triggered ROS production in 4 *NbKIN10* homolog silenced *N. benthamiana* expressing effector

Flg22-induced ROS burst was measured for 75 min from *N. benthamiana* leaf disks. GFP control and AvrPtoB were included as negative and positive control respectively. (A) kinetic of ROS production following elicitation with flg22. (B). Total ROS production for 75min was presented as relative (%) to GFP control. Data shown in (A-B) are means \pm SEM ($n=8$) from one independent experiment. RLU, relative light unit.

Discussion

Interactions between plant pathogens and their hosts are complicated and dynamic (Mukhtar et al., 2011). To understand these mechanisms, it is critical to understand protein-protein interaction between the pathogens and the host plants. One basic property of proteins is the ability to bind specific targets and/or form a non-covalent complex with other proteins (Ferro and Trabalzini., 2012). Yeast two-hybrid is an efficient way to identify and draw an interaction map between effectors from pathogens and plant proteins. In this study, *R. solanacearum* effector RipAO was used as bait in yeast two-hybrid screening to identify its targets and understand how it contributes to making the host plant a favorable environment for bacterial colonization. *R. solanacearum* has a large number of hosts including crops in *Solanaceae* family and one of the well-studied model plant *A. thaliana* (Genin and Denny., 2012). Therefore, in order to identify the interactors of RipAO in the plant, *A. thaliana* whole cDNA library was used. Through the Yeast two-hybrid screening, three interactors in *A. thaliana* SEC3A, KIN10, and OXA1 were identified as candidate interactors. Although three interactors were revealed through the screening, still there are some limitations. Firstly, the sequence fragments of the cDNA library are not complete. So RipAO may have more interactors in *A. thaliana*. It is because cDNA is synthesized from the 3' end to 5' end and usually the synthesis of them is not complete. Thus, proteins translated from the cDNA might have N-terminal missing fragments. Therefore, if the RipAO interacts with the domain at the N-terminal of interactors, screening may not be able to give all the interactors. Second, the cDNA library used for screening was from *P. syringae* infected *A. thaliana*. So,

it may not give the same result if the screening was performed with *R. solanacearum* infected *A. thaliana* cDNA library. Even though it may not give a complete protein-protein interaction map, still it gives clues to understand the mechanism of the RipAO. Although the yeast two-hybrid screening requires additional experiments such as co-expression *in planta*, the initial screening from yeast two-hybrid gives a lot of benefits to screening many proteins at the same time easily.

SEC3A

SEC3 is one of the exocyst complex components and was first found in the budding yeast (Terbush et al., 1996; Bushra et al 2019). There are two *SEC3* genes in *A. thaliana*, *SEC3A* and *SEC3B* (Chong et al., 2009). However, there are also two types of *SEC3A* (*ATIG47550.1* and *ATIG47550.2*) due to alternative splicing (Arabidopsis.org). While I was cloning the SEC3A cDNA, I could amplify both forms of SEC3A. Therefore, I cloned both forms of SEC3A into the yeast expression vector in order to test whether 654th Valine is affecting the interaction with RipAO. As a result of the yeast two-hybrid assay, I could observe that both forms of SEC3A are interacting with RipAO in yeast. This result may indicate that 654th Valine is not critical for RipAO in interacting with SEC3A. But it is still unknown about the functional difference between the two forms of SEC3A.

SEC3 is known to be critical for polarized exocytosis by mediating the interaction with phosphatidylinositol 4,5-bisphosphate (PI(4,5)P₂) in the plasma membrane (Finger et al., 1998; Hutagalung et al., 2009; Zhang et al 2013). Two domains in SEC3A, phosphatidylinositol 4,5-bisphosphate (PIP₂) domain (50-144aa) and SEC3_C-terminal domain (224-871aa) are involved in such SEC3A functions. First, the PIP₂ domain is close to N-terminal and is predicted to bind to the inner

leaflet of the plasma membrane (Bushra et al 2019). Second, the SEC3_C-terminal domain is close to the C-terminal of SEC3A and is predicted to be involved in polarized secretion (ebi.ac.uk/interpro/). In order to test which domain of SEC3A is interacting with RipAO, I generated truncated SEC3A N-terminal (1-471aa) and SEC3A C-terminal (471-889aa), respectively. Through the yeast-two hybrid assay, I could observe that SEC3A C-terminal is interacting with RipAO. This maybe indicates that RipAO inhibits the polarized secretion of unknown protein(s) in the vesicle.

In addition, to examine whether SEC3A is interacting with RipAO *in planta*, YFP-tagged SEC3A was co-expressed with FLAG-tagged RipAO in *N. benthamiana* leaves. Then the immunoblotting was performed with the total protein extract using anti-GFP and anti-FLAG antibodies. As a result of this, less SEC3A accumulation was observed in the presence of RipAO compared with the SEC3A co-expressed with PopP2-FLAG. This indicates that RipAO may interact with SEC3A *in planta* or at least modify SEC3A stability. SEC3A is a landmark protein that is involved in the recruitment of other exocyst subunits in the cytoplasm (Finger et al., 1998; Hutagalung et al., 2009; Zhang et al 2013). Maybe RipAO targets SEC3A to inhibit the recruitment of other exocyst subunits or to interfere with vesicle trafficking. RipAO may promote the degradation of SEC3A either directly or indirectly. There are some effectors reported to targets exocyst components. For instance, AvrPtoB of *P. syringae* pv. *tomato* (*Pto*) strain DC3000 mediates the degradation of exocyst component EXO70B1 via host 26S proteasome which requires E3 ligase activity (Wang et al., 2019). EXO70 family is one of the eight subunits of the exocyst complex and some of them in the EXO70 family are reported to be involved in plant

immunity (Zarsky et al., 2020). Another effector of Pto DC3000, HopM1 targets immune-related protein AtMIN7 and mediates degradation by the host's proteasome (Nomura et al., 2006). AtMIN7 is localized in the *trans*-Golgi network/early endosome (TGN/EE) and has a critical role in PTI and ETI (Nomura et al., 2011). As RipAO does not have any domains associated with proteasomal degradation, it is more likely that RipAO mediates the degradation indirectly such as ubiquitination of target protein by recruiting plant ubiquitin ligase to mediate proteasomal degradation or by autophagy. Therefore, to confirm whether the degradation of SEC3A is also mediated in the same manner, proteasome inhibitors such as MG132 and epoxomicin can be used for further study (Nomura et al., 2006; Wang et al., 2019).

VIGS has been used to provide important new insights into the role of specific genes in plant development and plant defense responses (Burch-Smith et al., 2004). Here I examined whether the SEC3A is required for the RipAO function. RipAO showed suppression of flg22-triggered ROS burst in *N. benthamiana* (Jeon et al., 2020). To test whether the interactors are required for RipAO, flg22-triggered ROS production was measured in two *NbSEC3A* homologs silenced *N. benthamiana*. In both *NbSEC3A* silenced plants, flg22-triggered ROS production was not suppressed or showed decreased suppression by RipAO. Therefore, taken these all the results, SEC3A is required for RipAO to suppress flg22-triggered ROS burst. Although all the results showed decreased suppression of total ROS by RipAO in both *NbSEC3A* silenced plants, the results from all the biological replicates were variable. This may be due to *SEC3A* was not completely silenced but partially expressed in the plants. In order to confirm whether complete knock-down of *SEC3A*

affects RipAO function, flg22-triggered ROS production should be measured in *A. thaliana SEC3A* knock-out mutant expressing RipAO.

KIN10

KIN10 is one of the SnRK1 (SNF1 related protein kinase) family and is known to act as a metabolic sensor (Hulsmans et al., 2016). SnRK1 is a protein kinase that is a putative regulator of sugar metabolism (Szczesny et al., 2010). In this study, through the yeast-two-hybrid screening, KIN10 was found as a second candidate interactor of RipAO. KIN10 was co-expressed with RipAO in *N. benthamiana* leaves to test whether it is associated with RipAO. Total proteins were extracted and immunoblotting was performed using two antibodies. As a result of the immunoblotting, KIN10-YFP was accumulated as much as the positive control LIP5 did. However, the result of co-IP using anti-FLAG antibody-conjugated beads indicate that RipAO did not interact with KIN10, which is distinct from what it showed in the yeast two hybrid assay. SNF1-related protein kinase is complex of three subunits, catalytic α , regulatory β , and γ subunits (Ghillebert et al., 2011; Hulsmans et al., 2016). The subcellular localization of SNF1 protein kinase is regulated by β subunits and known to localize to nucleus, vacuole and/or cytoplasm (Vincent et al., 2001). Therefore, KIN10 may not localize to the same region *in planta* and in yeast. Therefore, the interaction may not happen in plants. Although there was no direct interaction between KIN10 and RipAO, RipAO may require KIN10 for its role. Thus, to test whether KIN10 is required for RipAO suppression of flg22-triggered ROS production, four *NbKIN10* homologs silenced *N. benthamiana* were generated. Due to the high percentage of identity of four *NbKIN10*, three theoretical silencing fragments could be derived. Among 3 types of

silenced plants, only the plant infected with TRV:NbKIN10_4 could silence the corresponding gene. This may be caused due to the inefficiency of silencing fragment for NbKIN10_1-2 and NbKIN10_3 or the fragment may have knock-down off-targets. Interestingly, all the four NbKIN10 homologs were partially silenced in TRV:NbKIN10_4 infected plant. This seems to be due to identical 23 bp of the nucleotide sequence in NbKIN10_4 fragment with the others. Even though the 4 homologs were not fully silenced, likely, four NbKIN10 does not play a role in RipAO flg22-triggered ROS production. The data did not suggest any relevant result between RipAO and KIN10 *in planta*. But RipAO activity maybe requires another effector activity to be associated with KIN10. SnRK1 is known to be involved in the activity of two *Xanthomonas campestris* pv. *vesicatoria* (*Xvc*) effectors, AvrBs1, and AvrBst (Hulsmans et al., 2016). AvrBs1 is recognized by one of the R-protein of pepper, Bs1, and SnRK1 is required to trigger a hypersensitive response (HR) (Szczeny et al., 2010). Then, AvrBst can suppress AvrBs1-mediated HR (Szczeny et al., 2010). Maybe, similar to such a mechanism, RipAO can be involved in or suppress the other *R. solanacearum* effector-dependent HR. Moreover, SnRK1 was reported to interact with and destabilize barley WRKY3 transcription factor (TF) to enhance resistance to obligate biotrophic fungal pathogen *Blumeria graminis* f. sp. *hordei* (*Bgh*) (Han et al., 2020). Barley WRKY3 transcription factor interacts with WRKY1 and WRKY2 TFs which are the repressor of PAMP-triggered basal defense (Shen et al., 2007). Therefore, maybe RipAO interferes with the unknown interaction between SnRK1 and WRKY TF in *A. thaliana* to suppress immune responses.

OXA1

To test whether the third interactor OXA1 is interacting with RipAO, two proteins

were co-expressed in *N. benthamiana* leaf. Unfortunately, the OXA1-YFP was not accumulated enough to be detected by the anti-GFP antibody. This may be because the total protein extract condition was not optimal for the OXA1 due to its localization. OXA1 is a chaperone that is involved in protein sorting and folding, and localizes in mitochondria inner-membrane (Sakamoto et al., 2000). According to the previous study, RipAO was observed to be localized in the nucleus and vesicles through the confocal assay (Jeon et al., 2020). Taken these together, it is likely that RipAO and OXA1 are not localized in the same region of the plant cell. Therefore, OXA1 may not be the true interactor of RipAO.

Taken all these together, the compromised accumulation of SEC3A specifically in presence of RipAO suggests that SEC3A is the suitable interactor to understand RipAO activity. SEC3A is a landmark component to form an exocyst complex with other subunits and provides a polarized location of the vesicle. It seems that SEC3A would provide insight into how effector interferes with the vesicle trafficking for bacterial pathogens to colonize in the plants. Therefore, maybe the eventual function of RipAO can be blocking the polarized secretion of antimicrobials in the vesicle that SEC3A is leading.

REFERENCES

- Avila, J., Gregory, O.G., Su, D., Deeter, T.A., Chen, S., Silva-Sanchez, C., Xu, S., Martin, G.B., Devarenne, T.P.,** 2012. The beta-subunit of the SnRK1 complex is phosphorylated by the plant cell death suppressor Adi3. *Plant Physiol* **159**, 1277-1290.
- Bednarek, P., Kwon, C., Schulze-Lefert, P.,** 2010. Not a peripheral issue: secretion in plant-microbe interactions. *Curr Opin Plant Biol* **13**, 378-387.
- Ben Khaled, S., Postma, J., Robatzek, S.,** 2015. A moving view: subcellular trafficking processes in pattern recognition receptor-triggered plant immunity. *Annu Rev Phytopathol* **53**, 379-402.
- Benz, M., Soll, J., Ankele, E.,** 2013. *Arabidopsis thaliana* Oxa proteins locate to mitochondria and fulfill essential roles during embryo development. *Planta* **237**, 573-588.
- Burch-Smith, T.M., Anderson, J.C., Martin, G.B., Dinesh-Kumar, S.P.,** 2004. Applications and advantages of virus-induced gene silencing for gene function studies in plants. *Plant J* **39**, 734-746.
- Cao, F.Y., Yoshioka, K., Desveaux, D.,** 2011. The roles of ABA in plant-pathogen interactions. *J Plant Res* **124**, 489-499.
- Chong, Y.T., Gidda, S.K., Sanford, C., Parkinson, J., Mullen, R.T., Goring, D.R.,** 2010. Characterization of the *Arabidopsis thaliana* exocyst complex gene families by phylogenetic, expression profiling, and subcellular localization studies. *New Phytol* **185**, 401-419.

- Deslandes., L., Olivier., J., Peeters., N., Feng., D.X., Khounlotham., M., Boucher., C., Somssich., I., Genin., S.p., Marco., Y.,** 2003. Physical interaction between RRS1-R, a protein conferring resistance to bacterial wilt, and PopP2, a type III effector targeted to the plant nucleus. *PNAS* **100**, 8024–8029.
- Du, Y., Overdijk, E.J.R., Berg, J.A., Govers, F., Bouwmeester, K.,** 2018. *Solanaceous* exocyst subunits are involved in immunity to diverse plant pathogens. *J Exp Bot* **69**, 655-666.
- Ellinger, D., Voigt, C.A.,** 2014. Callose biosynthesis in *Arabidopsis* with a focus on pathogen response: what we have learned within the last decade. *Ann Bot* **114**, 1349-1358.
- Ferro, E., Tralbalzini, L.,** 2013. The yeast two-hybrid and related methods as powerful tools to study plant cell signaling. *Plant Mol Biol* **83**, 287-301.
- J.Feys., B., J.Moisan., L., Newman., M.-A., E.Parker, J.,** 2001. Direct interaction between the *Arabidopsis* disease resistance signaling proteins, EDS1 and PAD4. *The EMBO Journal* **20**, 5400-5411.
- Finger., F.P., Hughes., T.E., Novick., P.,** 1998. Sec3p Is a Spatial landmark for polarized secretion in budding yeast. *Cell* **92**, 559–571.
- Fu, Z.Q., Dong, X.,** 2013. Systemic acquired resistance: turning local infection into global defense. *Annu Rev Plant Biol* **64**, 839-863.
- Gao, M., Wang, X., Wang, D., Xu, F., Ding, X., Zhang, Z., Bi, D., Cheng, Y.T., Chen, S., Li, X., Zhang, Y.,** 2009. Regulation of cell death and innate immunity by two receptor-like kinases in *Arabidopsis*. *Cell Host Microbe*

6, 34-44.

Genin, S., Denny, T.P., 2012. Pathogenomics of the *Ralstonia solanacearum* species complex. *Annu Rev Phytopathol* **50**, 67-89.

Ghillebert, R., Swinnen, E., Wen, J., Vandesteene, L., Ramon, M., Norga, K., Rolland, F., Winderickx, J., 2011. The AMPK/SNF1/SnRK1 fuel gauge and energy regulator: structure, function and regulation. *FEBS J* **278**, 3978-3990.

Gu, Y., Innes, R.W., 2012. The KEEP ON GOING protein of *Arabidopsis* regulates intracellular protein trafficking and is degraded during fungal infection. *Plant Cell* **24**, 4717-4730.

Gu, Y., Zavaliev, R., Dong, X., 2017. Membrane trafficking in plant immunity. *Mol Plant* **10**, 1026-1034.

Hala, M., Cole, R., Synek, L., Drdova, E., Pecenkova, T., Nordheim, A., Lamkemeyer, T., Madlung, J., Hochholdinger, F., Fowler, J.E., Zarsky, V., 2008. An exocyst complex functions in plant cell growth in *Arabidopsis* and tobacco. *Plant Cell* **20**, 1330-1345.

Halford, N.G., Hey, S., Jhurrea, D., Laurie, S., McKibbin, R.S., Paul, M., Zhang, Y., 2003. Metabolic signaling and carbon partitioning: role of Snf1-related (SnRK1) protein kinase. *J Exp Bot* **54**, 467-475.

Han, X., Zhang, L., Zhao, L., Xue, P., Qi, T., Zhang, C., Yuan, H., Zhou, L., Wang, D., Qiu, J., Shen, Q.H., 2020. SnRK1 phosphorylates and destabilizes WRKY3 to enhance barley immunity to powdery mildew. *Plant Commun* **1**, 100083.

- Hann, D.R., Rathjen, J.P.**, 2007. Early events in the pathogenicity of *Pseudomonas syringae* on *Nicotiana benthamiana*. *Plant J* **49**, 607-618.
- He, Y., Wu, L., Liu, X., Zhang, X., Jiang, P., Ma, H.**, 2019. Yeast two-hybrid screening for proteins that interact with PFT in wheat. *Sci Rep* **9**, 15521.
- Huang, H., Ullah, F., Zhou, D.X., Yi, M., Zhao, Y.**, 2019. Mechanisms of ROS regulation of plant development and stress responses. *Front Plant Sci* **10**, 800.
- Hulsmans, S., Rodriguez, M., De Coninck, B., Rolland, F.**, 2016. The SnRK1 energy sensor in plant biotic interactions. *Trends Plant Sci* **21**, 648-661.
- Hutagalung, A.H., Coleman, J., Pypaert, M., Novick, P.J.**, 2009. An internal domain of Exo70p is required for actin-independent localization and mediates assembly of specific exocyst components. *Mol Biol Cell* **20**, 153-163.
- Jeon, H., Kim, W., Kim, B., Lee, S., Jayaraman, J., Jung, G., Choi, S., Sohn, K.H., Segonzac, C.**, 2020. *Ralstonia solanacearum* Type III Effectors with Predicted Nuclear Localization Signal Localize to Various Cell Compartments and Modulate Immune Responses in *Nicotiana* spp. *Plant Pathol J* **36**, 43-53.
- Jones, J.D., Dangl, J.L.**, 2006. The plant immune system. *Nature* **444**, 323-329.
- Kadota, Y., Sklenar, J., Derbyshire, P., Stransfeld, L., Asai, S., Ntoukakis, V., Jones, J.D., Shirasu, K., Menke, F., Jones, A., Zipfel, C.**, 2014. Direct regulation of the NADPH oxidase RBOHD by the PRR-associated kinase BIK1 during plant immunity. *Mol Cell* **54**, 43-55.

- Karkonen, A., Kuchitsu, K.,** 2015. Reactive oxygen species in cell wall metabolism and development in plants. *Phytochemistry* **112**, 22-32.
- Kawasaki, T., Yamada, K., Yoshimura, S., Yamaguchi, K.,** 2017. Chitin receptor-mediated activation of MAP kinases and ROS production in rice and *Arabidopsis*. *Plant Signal Behav* **12**, e1361076.
- Le Roux, C., Huet, G., Jauneau, A., Camborde, L., Tremousaygue, D., Kraut, A., Zhou, B., Levailant, M., Adachi, H., Yoshioka, H., Raffaele, S., Berthome, R., Coute, Y., Parker, J.E., Deslandes, L.,** 2015. A receptor pair with an integrated decoy converts pathogen disabling of transcription factors to immunity. *Cell* **161**, 1074-1088.
- Lozano-Duran, R., Bourdais, G., He, S.Y., Robatzek, S.,** 2014. The bacterial effector HopM1 suppresses PAMP-triggered oxidative burst and stomatal immunity. *New Phytol* **202**, 259-269.
- Lu, D., Wu, S., Gao, X., Zhang, Y., Shan, L., He, P.,** 2010. A receptor-like cytoplasmic kinase, BIK1, associates with a flagellin receptor complex to initiate plant innate immunity. *Proc Natl Acad Sci USA* **107**, 496-501.
- Macho, A.P., Zipfel, C.,** 2015. Targeting of plant pattern recognition receptor-triggered immunity by bacterial type-III secretion system effectors. *Curr Opin Microbiol* **23**, 14-22.
- Mei, K., Guo, W.,** 2018. The exocyst complex. *Curr Biol* **28**, R922-R925.
- Mittler, R.,** 2017. ROS are good. *Trends Plant Sci* **22**, 11-19.
- Nomura, K., Mecey, C., Lee, Y.N., Imboden, L.A., Chang, J.H., He, S.Y.,** 2011. Effector-triggered immunity blocks pathogen degradation of an immunity-

associated vesicle traffic regulator in *Arabidopsis*. Proc Natl Acad Sci USA **108**, 10774-10779.

Nomura., K., DebRoy., S., Lee., Y.H., Pumplin., N., Jones., J., He., S.Y., 2006. A bacterial virulence protein suppresses host innate immunity to cause plant disease. Science **313**, 220-223.

Pandey, S.P., Somssich, I.E., 2009. The role of WRKY transcription factors in plant immunity. Plant Physiol **150**, 1648-1655.

R.TerBush., D., Maurice., T., Roth., D., Novick., P., 1996. The exocyst is a multiprotein complex required for exocytosis in *Saccharomyces cerevisiae*. The EMBO Journal **15** 6483-6494.

Richardson, L.G.L., Singhal, R., Schnell, D.J., 2017. The integration of chloroplast protein targeting with plant developmental and stress responses. BMC Biol **15**, 118.

Saeed, B., Brillada, C., Trujillo, M., 2019. Dissecting the plant exocyst. Curr Opin Plant Biol **52**, 69-76.

Sakamoto., W., Spielewoy., N., Bonnard., G., Murata., M., Wintz., H., 2000. Mitochondrial localization of AtOXA1, an *Arabidopsis* homologue of yeast Oxa1p involved in the insertion and assembly of protein complexes in mitochondrial inner membrane. Plant Cell Physiol **41**, 1157–1163.

Sarris, P.F., Duxbury, Z., Huh, S.U., Ma, Y., Segonzac, C., Sklenar, J., Derbyshire, P., Cevik, V., Rallapalli, G., Saucet, S.B., Wirthmueller, L., Menke, F.L.H., Sohn, K.H., Jones, J.D.G., 2015. A plant immune receptor detects pathogen effectors that target WRKY transcription factors. Cell **161**,

1089-1100.

Segonzac, C., Newman, T.E., Choi, S., Jayaraman, J., Choi, D.S., Jung, G.Y., Cho, H., Lee, Y.K., Sohn, K.H., 2017. A conserved EAR motif is required for avirulence and stability of the *Ralstonia solanacearum* effector PopP2 *in planta*. *Front Plant Sci* **8**, 1330.

Segonzac, C., Zipfel, C., 2011. Activation of plant pattern-recognition receptors by bacteria. *Curr Opin Microbiol* **14**, 54-61.

Shen, Q.-H., Mauch, Y.S.S., Biskup, C., Bieri, S., Keller, B., Seki, H., Ülker, B., Somssich, I.E., Schulze-Lefert, P., 2007. Nuclear activity of MLA immune receptors links isolate-specific and basal disease-resistance responses. *Science* **315**, 1098-1103.

Stegmann, M., Anderson, R.G., Westphal, L., Rosahl, S., McDowell, J.M., Trujillo, M., 2013. The exocyst subunit Exo70B1 is involved in the immune response of *Arabidopsis thaliana* to different pathogens and cell death. *Plant Signal Behav* **8**, e27421.

Szczesny, R., Buttner, D., Escobar, L., Schulze, S., Seiferth, A., Bonas, U., 2010. Suppression of the AvrBs1-specific hypersensitive response by the YopJ effector homolog AvrBsT from *Xanthomonas* depends on a SNF1-related kinase. *New Phytol* **187**, 1058-1074.

Vincent, O., Townley, R., Kuchin, S., Carlson, M., 2001. Subcellular localization of the Snf1 kinase is regulated by specific beta subunits and a novel glucose signaling mechanism. *Genes Dev* **15**, 1104-1114.

Wang, F., Shang, Y., Fan, B., Yu, J.Q., Chen, Z., 2014. *Arabidopsis* LIP5, a

positive regulator of multivesicular body biogenesis, is a critical target of pathogen-responsive MAPK cascade in plant basal defense. *PLoS Pathog* **10**, e1004243.

Wang, W., Liu, N., Gao, C., Cai, H., Romeis, T., Tang, D., 2020. The *Arabidopsis* exocyst subunits EXO70B1 and EXO70B2 regulate FLS2 homeostasis at the plasma membrane. *New Phytol* **227**, 529-544.

Wang, W., Liu, N., Gao, C., Rui, L., Tang, D., 2019. The *Pseudomonas syringae* effector AvrPtoB associates with and ubiquitinates *Arabidopsis* exocyst subunit EXO70B1. *Front Plant Sci* **10**, 1027.

Wang, W.M., Liu, P.Q., Xu, Y.J., Xiao, S., 2016. Protein trafficking during plant innate immunity. *J Integr Plant Biol* **58**, 284-298.

Wei, Y., Sang, Y., Macho, A.P., 2017. The *Ralstonia solanacearum* type III effector RipAY is phosphorylated in plant cells to modulate its enzymatic activity. *Front Plant Sci* **8**, 1899.

Wu, B., Guo, W., 2015. The Exocyst at a Glance. *J Cell Sci* **128**, 2957-2964.

Zarsky, V., Sekeres, J., Kubatova, Z., Pecenkova, T., Cvrckova, F., 2020. Three subfamilies of exocyst EXO70 family subunits in land plants: early divergence and ongoing functional specialization. *J Exp Bot* **71**, 49-62.

Zhang, J., Shao, F., Li, Y., Cui, H., Chen, L., Li, H., Zou, Y., Long, C., Lan, L., Chai, J., Chen, S., Tang, X., Zhou, J.M., 2007. A *Pseudomonas syringae* effector inactivates MAPKs to suppress PAMP-induced immunity in plants. *Cell Host Microbe* **1**, 175-185.

Zhang, Y., Immink, R., Liu, C.M., Emons, A.M., Ketelaar, T., 2013. The

Arabidopsis exocyst subunit SEC3A is essential for embryo development and accumulates in transient puncta at the plasma membrane. *New Phytol* **199**, 74-88.

Zhang, Y., Liu, C.M., Emons, A.M., Ketelaar, T., 2010. The plant exocyst. *J Integr Plant Biol* **52**, 138-146.

Zhao, T., Rui, L., Li, J., Nishimura, M.T., Vogel, J.P., Liu, N., Liu, S., Zhao, Y., Dangl, J.L., Tang, D., 2015. A truncated NLR protein, TIR-NBS2, is required for activated defense responses in the *exo70B1* mutant. *PLoS Genet* **11**, e1004945.

Zhou, B., Zeng, L., 2017. Elucidating the role of highly homologous *Nicotiana benthamiana* ubiquitin E2 gene family members in plant immunity through an improved virus-induced gene silencing approach. *Plant Methods* **13**, 59.

Zipfel, C., 2014. Plant pattern-recognition receptors. *Trends Immunol* **35**, 345-351.

초 록

식물은 병원균에 대항하여 내재된 면역체계를 가지고 있다. 그래서, 많은 세균성 병원균들은 증식을 위해 이펙터(type III effectors, T3E) 단백질을 주입하며, 이펙터는 기주식물의 방어와 관련된 요소들을 타겟으로 한다. 이러한 이유로, 기주 식물에서 이펙터 단백질과 상호작용하는 단백질을 규명하는 것은 중요하다. 세균성 병원균의 하나인 *R. solanacearum*은 다양한 원예작물에 심각한 세균성 풋마름병을 일으킨다. *R. solanacearum*의 이펙터 중 하나인 RipAO는 담배 (*Nicotiana benthamiana*) 에서 식물의 방어 작용의 하나인 활성산소종 (reactive oxygen species) 생성을 억제한다. 본 연구에서는 애기장대(*A. thaliana*) cDNA 라이브러리에서 RipAO와 상호작용하는 단백질을 선별하여 이 단백질들이 RipAO의 담배의 활성산소종 생성을 억제하는 것과 연관성이 있는지 실험하였다. 효모 단백질 잡종법(yeast two-hybrid) 스크리닝 결과, 세가지의 단백질, exocyst complex component SEC3A (SEC3A), SNF1 related protein kinase (KIN10) 그리고 *Arabidopsis thaliana* homolog of yeast oxidase assembly 1 (OXA1)들이 RipAO와 상호작용하는 후보 단백질들로 발견되었다. 흥미롭게도, 담배에서 RipAO 존재 하에 SEC3A 단백질의 축적이 감소하는 것이 발견되었다. 또한 애기장대의 SEC3A의 homolog 단백질(NbSEC3A)들의 발현이 억제된 담배에서 RipAO가 활성산소종의 생성을 억제하지 못하는 것으로 확인 되었다. 이러한 결과들을 종합해 볼 때 RipAO는 SEC3A 단백질을 타겟으로 하며, SEC3A 단백질이 RipAO가 활성산소종을 억제하는데 필요한 요소로 밝혀졌다. 그러므로 본 연구에서는 기주 식물의 방어 작용을 억제하기 위해 막 수송 조직을 타겟으로 하는 이펙터 단백질을 규명하였다.

주요어: exocyst complex component SEC3A, SNF1 related protein

kinase, *Arabidopsis thaliana* homolog of yeast oxidase assembly 1, 효
모 단백질 잡종법(yeast two-hybrid), 활성산소종(reactive oxygen
species), *Ralstonia solanacearum*, 애기장대(*Arabidopsis thaliana*), 담
배(*Nicotiana benthamiana*)

학번: 2019-21592